Journal of Advanced Research 40 (2022) 69–94

Contents lists available at ScienceDirect

Journal of Advanced Research

journal homepage: www.elsevier.com/locate/jare

Review

Applying extrusion-based 3D printing technique accelerates fabricating complex biphasic calcium phosphate-based scaffolds for bone tissue regeneration

Nima Beheshtizadeh [a,e,†], Mahmoud Azami [a,e,†], Hossein Abbasi [b], Ali Farzin [c,d,e,*]

[a] Department of Tissue Engineering, School of Advanced Technologies in Medicine, Tehran University of Medical Sciences, Tehran, Iran
[b] Faculty of Mechanical Engineering, University of Tabriz, Tabriz, Iran
[c] Department of Applied Cell Sciences, School of Advanced Technologies in Medicine, Tehran University of Medical Sciences, Tehran, Iran
[d] Division of Engineering in Medicine, Department of Medicine, Brigham and Women's Hospital, Harvard Medical School, Cambridge, MA 02139, USA
[e] Regenerative Medicine Group (REMED), Universal Scientific Education and Research Network (USERN), Tehran, Iran

H I G H L I G H T S

- Biphasic calcium phosphates offer a chemically similar biomaterial to the natural bone, which can significantly accelerate bone formation and reconstruction.
- Robocasting is a suitable technique to produce porous scaffolds supporting cell viability, proliferation, and differentiation.
- This review discusses materials and methods utilized for BCP robocasting, considering recent advancements and existing challenges in using additives for bioink preparation.
- Commercialization and marketing approach, *in-vitro* and *in-vivo* evaluations, biologic responses, and post-processing steps are also investigated.
- Possible strategies and opportunities for the use of BCP toward injured bone regeneration along with clinical applications are discussed.

G R A P H I C A L   A B S T R A C T

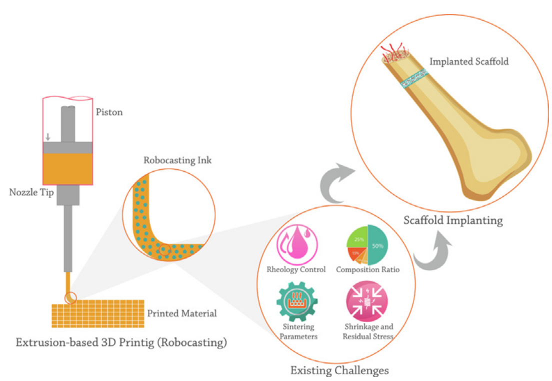

Abbreviations: AM, Additive manufacturing; ALP, Alkaline phosphatase; BJP, Binder jet printing; BCP, Biphasic Calcium Phosphate; BMSCs, Bone marrow stromal cells; BMP-2, Bone morphogenic protein 2; BTE, Bone tissue regenerating; CPO, Calcium peroxide; CaPs, Calcium phosphates; CAD, Computer-aided design; ELISA, Enzyme-linked immunosorbent assay; FEM, Finite element modeling; FDM, Fused deposition modeling; GelMA, Gelatin-methacryloyl; GNPs, Graphene Nanoplatelets; hAT-MSCs, Human adipose tissue-derived mesenchymal stem cells; hBMSCs, Human bone mesenchymal stem cells; hMSCs, Human mesenchymal stem cells; HA, Hydroxyapatite; IGF-1, Insulin-like growth factor-1; PDGF-AB, Platelet-derived growth factor-AB; PRF, Platelet-rich fibrin; PEG, Poly ethylene glycol); PMMA, Poly-methacrylate; PCL, Polycaprolactone; PLA, Polylactic acid; PLGA, Polylactic-co-glycolic acid; PVA, Polyvinyl alcohol; SLS, Selective laser sintering; SLM, Selective laser melting; SBF, Simulated Body Fluid; SLA, Stereolithography; SFE, Surface free energy; TRAP, Tartrate-resistant acid phosphatase; TIPS, Thermally-induced phase separation; 3D, Three-dimensional; TE, Tissue engineering; TGF- β1, Transforming growth factor- β1; TCP, Tri-Calcium Phosphate; TNF-α, Tumor necrosis factor; UDMA, Urethane di-methacrylate; VEGF, Vascular endothelial growth factor; β-CPP, β-Calcium Pyrophosphate; β-TCP, β-Tricalcium Phosphate.

Peer review under responsibility of Cairo University.

* Corresponding author at: Department of Applied Cell Sciences, School of Advanced Technologies in Medicine, Tehran University of Medical Sciences, Tehran, Iran (Ali Farzin).

E-mail address: afarzin@sina.tums.ac.ir (A. Farzin).

† These two authors are equally contributed in this work.

https://doi.org/10.1016/j.jare.2021.12.012
2090-1232/

• The study proposes that BCP possesses an acceptable level of bone substituting, considering its challenges and struggles.

A R T I C L E   I N F O

Article history:
Received 14 September 2021
Revised 9 December 2021
Accepted 23 December 2021
Available online 28 December 2021

Keywords:
Bone tissue engineering
Biphasic calcium phosphate
Extrusion-based 3D printing
Robocasting
Additive manufacturing

A B S T R A C T

Background: Tissue engineering (TE) is the main approach for stimulating the body's mechanisms to regenerate damaged or diseased organs. Bone and cartilage tissues due to high susceptibility to trauma, tumors, and age-related disease exposures are often need for reconstruction. Investigation on the development and applications of the novel biomaterials and methods in bone tissue engineering (BTE) is of great importance to meet emerging today's life requirements.
Aim of review: Biphasic calcium phosphates (BCPs) offer a chemically similar biomaterial to the natural bone, which can significantly promote cell proliferation and differentiation and accelerate bone formation and reconstruction. Recent advancements in the bone scaffold fabrication have led to employing additive manufacturing (AM) methods. Extrusion-based 3D printing, known also as robocasting method, is one of the extensively used AM techniques in BTE applications. This review discusses materials and methods utilized for BCP robocasting.
Key scientific concepts of review: Recent advancements and existing challenges in the use of additives for bioink preparation are critically discussed. Commercialization and marketing approach, post-processing steps, clinical applications, *in-vitro* and *in-vivo* evaluations beside the biological responses are also reviewed. Finally, possible strategies and opportunities for the use of BCP toward injured bone regeneration are discussed.

Introduction

Bone tissue engineering

Increasing the demand for life quality leads to developing the new converging technologies. Recent developments in science and technology promise a better future for humankind [1]. Tissue engineering (TE) is one salient example of these science and technology converging areas [2]. Restitution of the function and regeneration of the damaged tissues and organs could be considered the vision of TE while developing novel scaffolds that cells could survive on them is its mission [3].

Since bone is extensively faced with trauma, tumors, and age-related diseases, such as osteoporosis and osteoarthritis, there is currently a demand for an effective treatment method. Even though healthy bone tissues have the high regenerative ability, patients with primary diseases, such as those with diabetes or poor nutrition, suffer from prolonged bone regeneration procedures [4].

Significant bone defects emerging from genetic malformations, infections, surgical resection, or trauma maintain a considerable challenge for clinicians [5-7]. During the last years, clinical treatments based on replacing the lost bone tissue with autogenous bone grafts, allogeneic banked bone, xenogeneic sources, and synthetic bone substitutes have been developed [8,9]. However, each method has its advantages and disadvantages, leading to limited structural and functional recovery [10]. To remove the limitations of usual treatment methods of bone injuries, comprehensive strategies have been developed [11-13]. One of them is fabricating engineered constructs to promote bone regeneration.

One of the most fundamental objectives of TE is to produce functional constructs for damaged tissues [14]. Multiple three-dimensional (3D) scaffolds have offered temporary skeleton for new tissue ingrowth [11]. On the other hand, several requirements should be met by a developed scaffold to cause the restoration of the native tissue structure and function [15]. Biocompatibility, biodegradability, mechanical characteristics, the amount and size of porosities, and surface charge are primary factors for modifying cell adhesion and proliferation, diffusion of nutrients and gases on the surface of developed scaffolds, and subsequently assuring the success of tissue regeneration [16,17]. Appropriate scaffolds for bone regeneration applications possess some characteristics, including highly bioactive and degradable, along with 3D interconnected porous architecture and matched mechanical-loading ability [18].

The use of the appropriate biomaterial to provide biocompatibility and biodegradability of the scaffold would result in success in the subsequent stages of tissue growth [19]. Scaffolds should meet certain requirements in terms of each target tissue's status and cellular functions, such as having enough interconnected porosities, biological properties, and the ability to mimic the natural mechanical and physical properties of tissues [20].

Since targeted tissues need appropriate growth factors (GFs) and nutrients, constructed scaffolds should serve as a suitable cell development niche [21]. GFs regulate tissue morphogenesis, angiogenesis, and neurite outgrowth in development, while in adults, they play a decisive role in tissue healing and homeostasis [22]. GFs, like proteins and steroid hormones, play a significant role in controlling cellular function by acting as signaling molecules and binding to cell transmembrane receptors, greatly promoting cell ingrowth, proliferation, and differentiation [23,24]; however, scaffold preparation is still a challengeable discussion in BTE [25]. This study aims to cover recent advancements and current challenges focusing on extrusion-based 3D printing (as a novel way of developing complicated bone constructs) for the engineering of BCP (as a potential material for inducing osteogenesis and promoting bone regeneration) structures. Using various additives for bioink preparation, the strategy to commercialization and marketing, post-processing operations, clinical applications, and potential future prospects are all discussed.

Materials used in BTE

Analyzing the bone structure would lead our attention to the best compatible scaffold. It has been demonstrated that almost 60–70% of the dry mass of bone is the mineral part, which is mainly dedicated to hydroxyapatite (HA, $Ca_{10}(PO_4)_6(OH)_2$) [26]. Most of the rest is collagen, along with other substances like proteins and inorganic salts. Additional elements like silicon, carbonate, and zinc in various bone mineral causes the Ca: P ratios ranging from 1.37 – 1.87; whereas, HA possesses a constant Ca: P ratio of 1.67 [26].

Many researchers have devoted studies to developing the best-matched bone tissue scaffolds [27-30]. A wide range of biomaterials, such as polymers, ceramics, and hydrogels, have a great potential ability for employing in BTE [31]. Polylactic Acid (PLA) [32,33], Polylactic-co-glycolic Acid (PLGA) [34,35], Polycaprolactone (PCL) [36-38], HA [39-41], β-Tricalcium Phosphate (β-TCP) [42-44], Gelatin-Methacryloyl (GelMA) [45,46], BCP [47-49], and composites [50-54] are the most used biomaterials in BTE due to their acceptable mechanical and cell-friendly properties. Even though many efforts have been made to modify the composition of employed bone scaffolds, reaching a well-adapted composition in BTE has been a matter of discussion, in recent years. Kindly note that calcium phosphate-based bone substitutes are well-received by researchers and clinicians [55].

Calcium phosphate-based bone substitutes

Mineral calcium phosphates (CaPs) mainly contain calcium cations unitedly with orthophosphate, metaphosphate or pyrophosphate anions, and sometimes hydrogen or hydroxide ions [56]. CaPs, in the form of neat [57] or composite [29,58] scaffolds, are now at the center of the researchers' attention for use in BTE applications due to their biological and physical properties and similarities to the natural bone composition [3,52,59].

One of the attractive functional composites is the composition of HA with other Calcium Phosphate-based materials like Tricalcium Phosphate (TCP). TCP has three polymorphs: β-TCP (rhombohedral), α-TCP (monoclinic), and α'-TCP (hexagonal) [60]. The last two types are high-temperature forms; whereas, the former has a broad application in the biomedical fields. The composition of β-TCP and HA is also a kind of Calcium Phosphate ceramic called Biphasic Calcium Phosphate (BCP) with high similarity with bone mineral composition [61].

BCP scaffolds can be developed as bone substitutes in personalized shape and geometry through traditional like replica molding [62] and advanced like additive manufacturing (AM) [63] techniques. Utilizing AM methods in fabricating BCP-based bone constructs is a controversial method (Fig. 1) [64]. Variety in employed composition ratio, processing method, and environmental conditions lead to the salient differences in mechanical properties, pore size, cell responses, and consequently bone formation ability of fabricated constructs by AM technique [65].

Commercial concept of BCP

Given the current high growth in BTE requirements, producing an ideal material that meets the majority of the criteria would have the potential for commercialization by regenerative medicine firms. Based on the literature, BCP composition positively correlates with commercialization principles, considering a variety of composition ratio, porosity, and structure, resulted in various mechanical and biological performance [66]. High similarity of the biological [61] and mechanical properties [67] of BCP constructs to the natural bone tissue evoke the undeniable fact that BCP possesses the potential of commercialization and being available in the market. On a lighter note, the bench's progression to the bedside process is expected due to the effective application of BCP and its structures in multiple bone repair and dentistry applications [68].

Market evaluation illustrates that commercialized BCP is available with the HA: β-TCP ratio of 70: 30 to 60: 40 in powder, dense, and porous bulk forms [69] (Table 1). Osteon™ II (Dentium, USA) (HA: β-TCP ratio of 30: 70 and 250 μm sized porosities), is an evident BCP product that is gracious, especially in maxillary sinus augmentation. Excellent wettability and highly resorbable properties due to higher β-TCP content are its key features. The most application of Osteon™ II is in oral issues, such as periodontal defects, cystic cavities, extraction socket grafting, ridge augmentation, and sinus lift, while it also has orthopedic surgery applications [70].

MBCP® (Biomatlante, France), MBCP+® (Biomatlante, France), Triosite® (Biomatlante, France), and GENESIS-BCP™ (Dio Implant, South korea) are other commercialized BCP products available in the market [71,77]. MBCP® has a HA: β-TCP ratio announced by the manufacturer of 60: 40; whereas, MBCP+® has a ratio of 20: 80. Granules geometry was reported as 0.5–1 mm for both mentioned ones [71]. Miramond *et al.* [71] reported an elevated similarity ratio between MBCP® and MBCP+® scaffolds, utilizing them in preclinical studies. They showed that the geometry and morphology of granules, as well as grain size and macro- and microporosities, are homogenous.

In addition, the efficiency of the Triosite® bone graft substitute was critically evaluated in a prospective randomized study involving 341 patients undergoing posterior spinal fusion with associated instrumentation [78]. Triosite® possesses a HA: β-TCP ratio of 60: 40, and pore size of 300–600 μm for macropore and approximately under 10 μm for micropore structures [74]. Moreover, GENESIS-BCP™ has a HA: β-TCP ratio of 53.4: 43.6 with 65.5% porosity, 84.9% crystallinity, and Ca: P ratio of 1.61 [75].

Besides, for fussier handling in orthopedic surgeries, the mixture of hydrogel and BCP is preferred, which forms a new product that can be an appealing issue for active firms in this field. In'Oss™ (Biomatlante, France) is an injectable bone substitute that includes HA, β-TCP, and a kind of well-handling hydrogel [71]. In'Oss™ is a moldable bone graft that can fit into various grafting sites by keeping the original graft geometry. It is easy to use with no pre-mixing or required preparation. Its sticky viscosity allows easy positioning, along with adapting quickly to the shape of the defect. Exemplary contact with the bone surface and maximizing the bone-implant interface is another advantage of In'Oss™ [76]. In'Oss™ is recommended for socket preservation after tooth extraction and furcation defects. Its application around the implant during immediate implantation is possible due to its high shape-ability which can surround complicated-shape implants [76].

Methods for the fabrication of bone tissue scaffolds

Various scaffold fabricating methods have been developed depending on the property of targeted tissue, usability, viability, type of materials, surface topography, porosity volume, mechanical properties, and production scale [79]. Here, we consider traditional methods and recent advancements in BTE scaffolds fabrication.

Methods for the fabrication of polymer-based scaffolds

Solvent casting and particulate leaching [80], gas foaming [81], emulsion freeze-drying [82], electrospinning [83,84], thermally induced phase separation (TIPS) [85], and AM [86] methods are used to produce polymeric-based bone scaffolds. Solvent casting is a simple and most generally used technique for the fabrication of 3D polymeric scaffolds through mixing water-soluble salts like Sodium Chloride and Sodium Citrate particles into a biodegradable polymer solution and casting into a mold with a desired shape [13]. Solvent removal via evaporation or lyophilization leads to leaching out the salt particles to achieve a porous structure (Fig. 2a) [13].

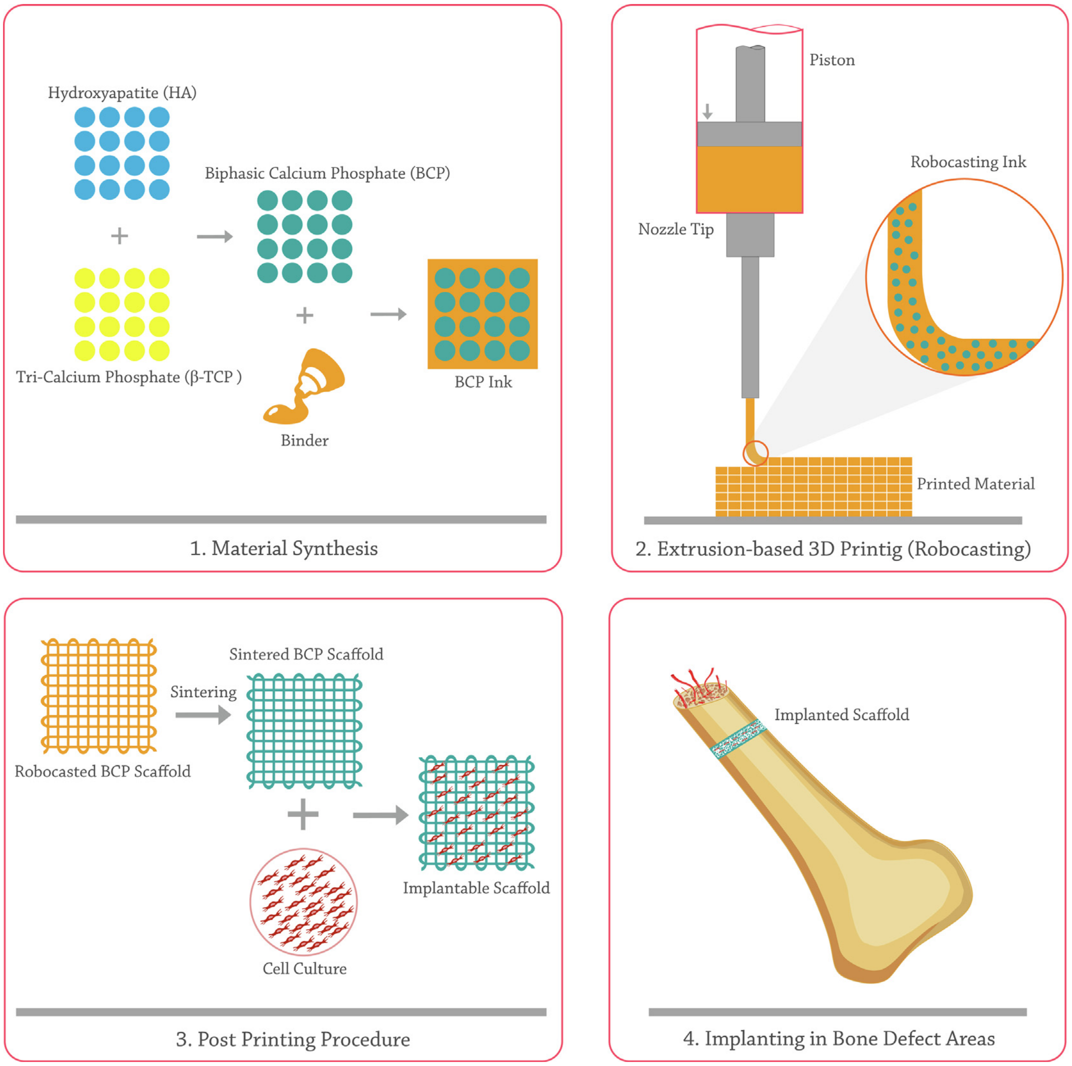

Fig. 1. A schematic of BCP robocasting steps and its application in bone regeneration.

Table 1
Most prevalent BCP products available in market.

BCP product	HA: β-TCP composition ratio	Manufacturer & Country	Granule's size	Ref.
Osteon™ II	30:70	Dentium, USA	0.2–2 mm	[70]
MBCP®	60:40	Biomatlante, France	0.5–1 mm	[71]
MBCP+®	20:80	Biomatlante, France	0.5–1 mm	[71]
Ceraform	65: 35	Teknimed, France	3 mm	[68]
Interpore200	–	Interpore, USA	0.425–1 mm	[72,73]
Triosite®	60:40	Biomatlante, France	0.5–4 mm	[74]
GENESIS-BCP™	60:40	Dio Implant, South korea	0.1–2 mm	[75]
In'Oss™	–	Biomatlante, France	–	[76]

Gas foaming is a technique for fabricating synthetic scaffolds that avoids the use of solvents [87]. High-temperature compression molding of the polymer into a solid disc is the first step of the procedure. The solid polymer rests in a high-pressure Carbon dioxide chamber for several days after the disc is formed. Throughout this time, the gas infiltration makes a porous structure (Fig. 2b) [88]. An advantage of gas foaming is the absence of caustic solvents. Hence, the presence of residual compounds in the final scaffold is not a main concern, in this technique. The possibility of incorporation of bioactive molecules in the fabricated structure is another advantage of using gas foaming method [87].

The electrospinning technique was developed since 2012, for preparing continuous fibers with the diameter in the range of sub-micron to nanometer [89]. Electrospinning depends on the high electrostatic forces, leading to producing fibers using just a solvent, which can disperse nanoparticles and dissolve the polymer (Fig. 2c). This method is employed to assemble nanofibers of polymers [90], metals [91], ceramics [92], and composites [93].

Hekmati *et al.* [94] revealed that the distance of needle tip to collector significantly affected the diameter of nanofibers made by electrospinning method. Their results indicated that reducing the distance of needle tip to the collector led to raising the diameter of the electrospun nanofibers. Moreover, polymer concentration, solution viscosity, flow rate, electric field intensity, and air humidity are some effecting parameters on the final fibrous scaffold [89].

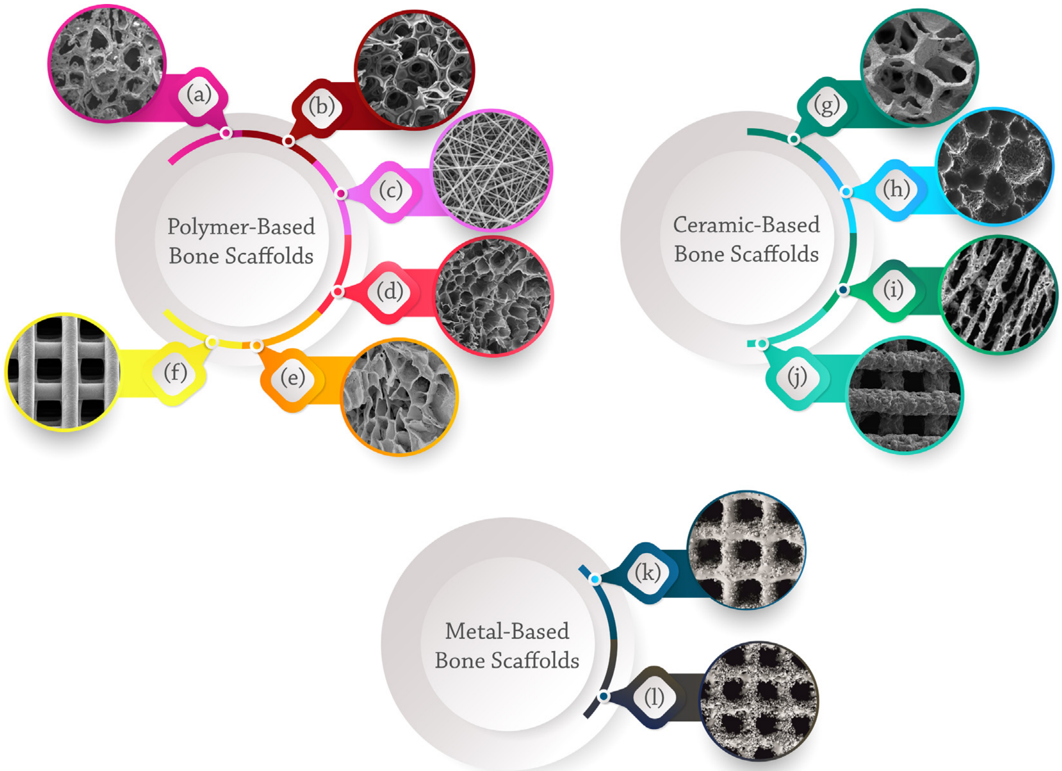

Fig. 2. SEM images of (a-f) polymeric and (g-j) ceramic scaffolds prepared by various methods: (a) PLGA-based scaffold with 92.38% porosity prepared by solvent casting and particulate leaching method, reproduced with permission from [258] (b) Gelatin-based scaffold with 85% porosity, prepared by gas foaming method, reproduced with permission from [259] (c) Gelatin/Glycosaminoglycan-based scaffold with a composition ratio of 90/10, prepared by electrospinning method, reproduced with permission from [260] (d) Gelatin-based scaffold crosslinked via acetone–water solution (4:1 v/v) containing a water-soluble EDC, prepared by freeze-drying method, reproduced with permission from [261] (e) PCL/ PLA/ gelatin nanofibers/ Taurine scaffold with a composition ratio of 1:1:0.4:0.01, prepared by thermally induced phase separation technique, reproduced with permission from [262] (f) PCL-based scaffold with square pore geometries and regular dimensions of 500 μm × 500 μm, prepared by 3D printing technique, reproduced with permission from [263] (g) Bio-glass/ Polyurethane-based scaffold, with 93 % porosity, prepared by replica method, reproduced with permission from [264] (h) BCP-based scaffold with a HA: β-TCP ratio of 1: 1, prepared by direct foaming method, reproduced with permission from [265] (i) HA-based scaffold with 47% porosity, prepared by freeze-casting method, reproduced with permission from [104], and (j) $Li_2Ca_4Si_4O_{13}$ scaffold with a controlled pore size of 250 μm, prepared by 3D printing method, reproduced with permission from [266], (k) Ti6Al4V-based bone scaffold fabricated via SLM method, reproduced with permission from [267], (l) Titanium-based bone scaffold fabricated via SLS method, reproduced with permission from [268]. All mentioned scaffolds have been successfully used in BTE applications, while the 3D printed ones possess superior results compared to other bone scaffolds.

Freeze-drying, also called "lyophilization", is a drying method through solidifying by freezing following solvent evaporation by sublimation upon heating [95]. Sublimation includes direct evaporation and condensation of a solid without forming an intermediary liquid phase [96]. During the process, the product loses more than 90% of its initial water. The transformation of the solid to the gas phase occurs without water and solvent passage through the liquid state [95]. Fig. 2d shows a SEM image of freeze-dried Gelatin-based scaffold crosslinked via Acetone–water solution (4:1 v/v) containing a water-soluble EDC.

A wide variety of porous constructs, especially polymeric membrane, can be fabricated via thermally-induced phase separation (TIPS) technique [85]. Fig. 2e demonstrates a PCL/ PLA/ Gelatin nanofibers/ Taurine scaffold with a composition ratio of 1:1:0.4:0.01 prepared by TIPS technique. In this way, a kind of polymer acts as a solvent and is casted in the form of film at a high-temperature. The polymer is dissolved by heating the mixture approximately near 60̊C for two hours in the solution, which consists of water and 1, 4-dioxane, while other components' dispersion, like Hydroxyapatite and Calcium Phosphates, could be applied through ultrasonication [85]. The homogeneous solution should then be heated to 15̊C above the measured cloud point temperature that the polymer solution becomes turbid. Final porous structure will be yielded by cooling the solution down to the quenching temperature obtained by a ramp temperature profile and removing the extra solvent [85].

However, mentioned traditional scaffold fabricating methods have some limitations in developing efficient bone scaffolds. Solvent casting and particulate leaching lead to a product with limited degree of pore size. Gas foaming is a moderately expensive method, and demands a series of equipment, while it is also limited to specific polymers such as PLGA, PCL, PLA, and poly (ethylene glycol) (PEG). Meanwhile, freeze-drying technique needs high capital cost of equipment and energy cost, along with lengthy processing time. It takes typically 36–72 h per each drying cycle [97]. Due to high applied pressure during freeze drying method, there are some possible damages to products due to the changes in pH and tonicity. Moreover, achieving fibrous structures with low mechanical performance and containing residual solvent are essential disadvantages of electrospinning technique.

All limitations lighten up using AM techniques in bone scaffold preparation, due to its application in a wide range of polymers, ceramics, and metals [98,99]. Stability, model reproducibility, and the architecture control ability of 3D scaffolds are the primary superiority of AM techniques, leading to improved biological and mechanical performances of tissue-engineered constructs [100]. Fig. 2f shows a 3D printed scaffold, which possesses a high porosity and internal interconnectivity.

Methods for the fabrication of ceramic-based scaffolds

Todays, ceramic-based bone scaffolds are prepared through conventional and advanced techniques. Conventional methods for making porous bone substitutes mainly include replica and sacrificial template, freeze-casting, and direct foaming methods [12]. A synthetic or natural template, which is impregnated with a ceramic suspension, was engaged in the replica method [101]. Missing template after drying leads to creating a replica of the primary template structure. Numerous synthetic and natural cellular structures could be hired as templates to produce macroporous ceramics through this technique. A high porosity rate scaffolds, based on ceramic/polymer blends could be prepared by the replica method. Fig. 2g shows a bio-glass/polyurethane-based scaffold with 93% porosity, possessing high interconnectivity, which is considered essential in ameliorating the cell activity and viability.

The sacrificial template method causes the obtaining of porous substitutes representing a negative replica of the original sacrificial template instead of the replica technique's positive morphology [102]. This method consolidates some pore former or sacrificial material to act as a place holder within the ceramic powder or slurry.

In the direct foaming method, gas bubbles are incorporated into a ceramic suspension. By setting and drying the slurry, the ceramic retains the resulting spherical pores [101]. Dried constructs are sintered at high temperatures to obtain high-strength ceramic scaffolds. The total porosity of the obtained foam is comparable to the amount of gas incorporated into the suspension or liquid medium during the foaming process [102]. Fig. 2h demonstrates an SEM image of a BCP-based scaffold with a HA: β-TCP ratio of 1: 1, prepared by the direct foaming method. The vacancies of gas bubbles are seen in these scaffold types, while they could prepare an appropriate area for enhancing cell attachment [103].

The freeze-casting technique is also used for the preparation of ceramic-based bone scaffolds [104]. In this technique, ceramic slurry is flowed into a mold and then frozen. Upon demolding, the frozen solvent temporarily plays as a binder and hold the ceramic particles together. Afterward, to purify the solvent under vacuum, the sample is freeze-dried. The freeze-drying method prevents drying stresses and shrinkage that may cause cracks and warping during regular drying. Sintering the freeze-drying products would lead to a porous construct with improved strength, stiffness, and desired porosity. The result is a ceramic-based bone scaffold with a complicated and usually anisotropic porous microstructure generated through the freeze-casting technique. A Hydroxyapatite-based scaffold with 47% porosity prepared by the freeze-casting method is shown in Fig. 2i.

It has been reported that AM methods are superior techniques in the field of both polymeric- and ceramic-based scaffolds fabrication [21]. The amount of interconnected porosities of ceramic-based scaffolds, which is a significant parameter in BTE, could be easily tuned through 3D printing method. Fig. 2j illustrates a ceramic-based bone scaffold with controlled pore size, square pore geometries and regular repeatable dimensions prepared by 3D printing method.

Methods for the fabrication of metal-based scaffolds

The most applicable bioinert metals used in bone implants and scaffold applications include Titanium alloys, Ti6Al4V, Cobalt-Chrome (CoCr) alloys, and 316L stainless steel [105]. Titanium and its alloys could be used as appropriate bone scaffolds since they are high-strength, bioinert, not biodegradable, and possess low density and modulus of elasticity [106]. Due to the outstanding corrosion resistance and biomechanical capabilities, Ti6Al4V is the most commonly used titanium alloy in orthopedics [107]. However, the osteointegration of Ti6Al4V is unsatisfactory because of its bioinert and high elasticity properties, which may limit early bone-implant attachment and long-term stability, resulting in aseptic loosening and providing a challenge to its widespread usage [108].

CoCr alloys have widely been employed in prosthetic arthroplasty. Their mechanical characteristics seem to make them a desirable material for total hip and knee joint arthroplasty [109]. Recent investigations, however, have highlighted some concerns about the osteogenic activity of the CoCr alloy, which may result in the loosening of arthroplasty employing this alloy [110]. Among the several types of metallic implants, the most popular bone-implant material is the surgical grade 316L stainless steel, which has strong mechanical properties, a relatively low cost, and widely availability [111]. However, the release of metal ions, such as iron, nickel, and chromium, in the biological environment is the most serious disadvantage of 316LSS biomedical applications [112].

Bone scaffolds could be fabricated from all the mentioned metallic biomaterials through selective laser melting (SLM) and selective laser sintering (SLS) techniques. SLM is an AM technique that uses a high-power-density laser to melt and fuse metallic powders. The SLM technique is based on the application of extremely thin layers of metallic powders to construct a platform, which are then totally melted by the heat energy caused by one or more laser beams (Fig. 2k) [113]. SLS is a powder-based AM process that employs laser light to melt and fuse powders, which are then stacked layer by layer to build a printed object based on 3D model data. Powder design and preparation have the substantial impact on the performance of SLS sintered components [114]. Even though the powdered material is melted in SLM, the working temperature in SLS method is below melting point. When a laser heats a powder material below its melting point, it fuses to produce a solid. The operating concept of both printing methods is almost the same (Fig. 2l).

A primary issue in utilizing metallic scaffolds is implant loosening, which is caused by the failure of an implant surface to integrate with the surrounding bone and other tissues owing to micromotions [115]. Another crucial element of the usage of metallic alloys in bone applications is osseointegration (the implant ability for integration to the bone and other tissue). To assure the implant's safety and effectiveness throughout its expected lifetime, it must be well integrated with the bone. A previous study [116] has demonstrated that increasing the roughness or performing other surface treatments may improve the bone response to implant surfaces [117]. Although the exact molecular processes are unknown, it is apparent that the surface's chemical and physical qualities influence implant–surface interactions through regulating cell activity, growth factor production, and osteogenic gene expression [118].

An available cost-effective strategy to cover the mentioned issues is coating the prepared metallic scaffold via ceramic slurries to increase the scaffold interaction and integrate with the bone and other surrounding tissues. Calcium Phosphate ceramics could be suitable for this application since they could interact appropriately with surrounding tissues. It was shown that HA has osteoconductive capabilities and that mechanical fixation of HA-coated implants was superior to uncoated implants under ideal surgical conditions [119]. Recently, researchers reported that coating the BCP on Ti6Al4V-based scaffolds significantly impacted their behavior in physiological medium, namely their dissolution-precipitation and corrosion protection capabilities [120].

Methods for the fabrication of composite scaffolds

Uncomplicated composite bone substitutes could be prepared by the described methods above, while complex structures need

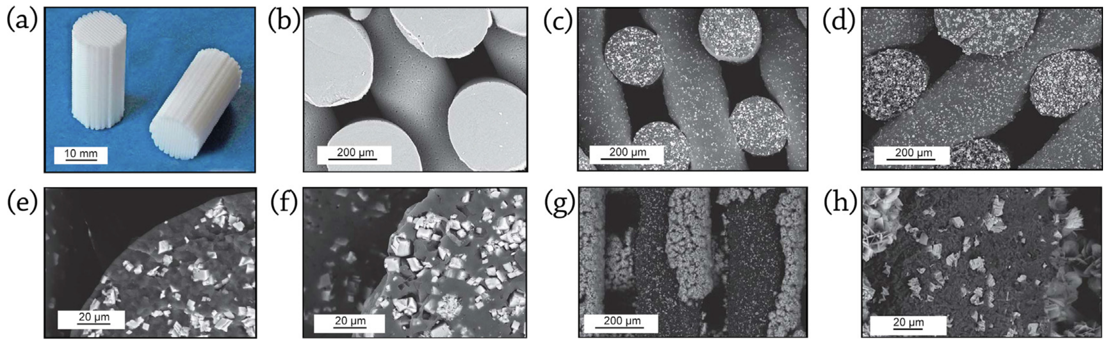

Fig. 3. 3D printing is an appropriate technique for preparing ceramic/polymer-based scaffolds. 3D printing of PCL-$CaCO_3$ composite bone scaffolds: (a) prepared scaffolds via 3D printing. SEM images of the (b) pure PCL (c) PCL-33 wt% $CaCO_3$ (d) PCL-50 wt% CaCO3. SEM images of the magnified cross-sections material contrast mode of (e) PCL-33 wt % $CaCO_3$ (f) PCL-50 wt% $CaCO_3$. (g, h) Bio-mineralization over 20 days in phosphate buffered saline (PBS)-Lipase. All images are reproduced with permission from [269].

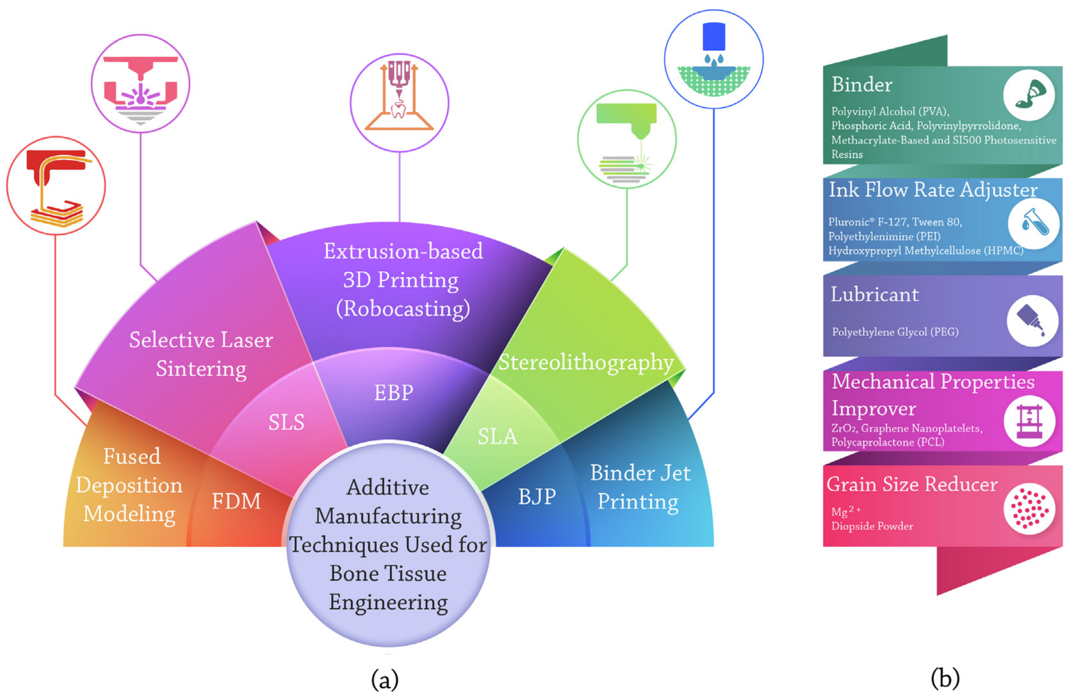

Fig. 4. (a) Additive manufacturing techniques for preparing 3D bone tissue scaffolds, including FDM, SLS, EBP, SLA, and BJP methods (b) Ink preparation materials and efficient additives for BCP robocasting, including binder, ink flow rate adjuster, lubricant, mechanical properties improver, and grain size reducer.

some accurate techniques. The composition of polymer and ceramic is desirable for BTE applications, while 3D printing is an appropriate technique to prepare these scaffolds. Fig. 3a and b show 3D printing of PCL-$CaCO_3$ composite bone scaffolds. The amount of ceramic in polymer content could be variable (Fig. 3c-f), while their biological behavior, including bio-mineralization in phosphate buffered saline (PBS)-Lipase are different (Fig. 3g-h). It should be noted that emerging novel methods in the engineering fields such as AM and rapid prototyping widen the converging technologies avenue, especially in health-related sciences [64]. Hence, to accomplish personalized medicine and produce specialized engineered tissues, AM techniques are useful [64].

A majority of bone tissue-specialized scaffolds are prepared via AM techniques (Fig. 4a). Stereolithography (SLA) [121,122], SLS [123,124], fused deposition modeling (FDM) [125,126] and binder jet printing (BJP) [127,128] have been used for composite bone scaffold fabricating, in recent years. SLA, which is called photo-solidification, is the procedure of model manufacturing via photochemical activity, causes forming polymers from cross-linking monomers and oligomers [129]. The main limitation of this method is developing functional photopolymerizable hydrogels for BTE.

In the SLS method, laser energy source is engaged to melt the polymer and ceramic powders. Like any other technique, SLS possesses some advantages and disadvantages. Manufacturing capability of great functional bone scaffolds with complicated geometry, along with an elevated level of accuracy, are its advantages. However, its accuracy is not as high as SLA. Moreover, due to the lack of support, the selective laser sintering of samples saves printing and post-processing time. Preparing powder-based models and scaffolds via SLS method is prevalent in BTE, while the non-powder forms are not appropriate candidates for this technique [123].

The extrusion process of heated feedstock plastic filaments through a nozzle tip is called fused deposition modeling (FDM), one of the most widely used AM techniques for preparing prototypes in conventional engineering plastics [130]. In FDM, the nozzle size affects resolution of fabricated constructs. Nozzle clogging is a common phenomenon in FDM technique, which may significantly affect its efficiency. Also, the main concern of FDM method is that the upper layers may deform the lower ones and destroy the fabricated structure [131]. While it is suggested to utilize FDM technique in a ventilated environment due to the heating feedstock plastic and its gases, FDM printers and used materials are very affordable, in which high-quality constructs could be manufactured via the FDM technique due to the accurate control and considerable production speed.

In the binder jet printing (BJP) method, a liquid binding material is selectively deposited via moving the inkjet print head across the powder's bed. Then a thin layer of powder is spread across the completed section. This process is repeated with each layer until the whole model is printed [132].

Since the fabricated constructs via the BJP method do not require any mechanical support, less materials are used in the BJP method, compared with FDM and SLA techniques [133]. Hence, the time needed for post-processing processes is lessened. Moreover, since all of the unused powder can be reused in future works, BJP is more economical. This fact comes more attractive, while in other techniques, such as SLS, only approximately 50% of unused material is re-usable [134].

Unlike the FDM technique, there is no warping or shrinking due to the differential cooling in the BJP method as it does not use heat. However, poor mechanical property of final product is the limitation of the BJP technique [135]. Even with sintering, samples created via BJP are not as persuasive as samples prepared with either SLS or FDM techniques.

Mentioned AM techniques, as well as extrusion-based 3D printing [18] are recommended facilities in achieving a person's bone defect geometry via fabricating and implanting a specified scaffold [136]. However, each one maintains its fascinating benefits, making it difficult to choose a suitable one that provides constructs with high physical and mechanical similarity to the target tissue [137]. Meanwhile, extrusion-based 3D printing method, known as robocasting, is one of the AM methods that directly prints an ink from a paste-like material. This paste-like material could be a polymer or some ceramic particles in viscose slurry. Adjusting its viscosity needs to try various conditions, altering the additive amounts [64].

Robocasting could be considered as a capable method for fabricating scaffold in TE, due to the high precision in the manufacturing process [138], lack of powder bed [139], the capability of fabrication of complicated structure [140], and lack of need to post-processing operation [139]. With the help of computer-aided design (CAD), the software can slice the model [141] and the printer machine lead to generate 3D structures layer by layer. The material flow is caused by a pneumatic system, a piston, or a screw. However, the recent models of precise printers enjoy from a ball screw mechanism that translates rotational motion to the linear one [142]. Due to the high potential of the robocasting method in the fabricating, complex bone scaffolds could be prepared by this strategy.

This paper aims to review the published reports on the robocasting of BCP and discuss the undeniable potential of BCP in regenerating bone tissue. To the best of our knowledge, there is not any review of robocasting of BCPs to date; whereas, its biological properties are well-known in this area. It is forecasted that utilizing these techniques will improve human life quality via developing all human tissue scaffolds [143].

Preparation of BCP bone scaffolds via robocasting technique

To discuss fabricating BCP bone scaffolds via the robocasting technique, it is necessary to describe green body scaffold fabricating, appropriate ink preparation, and effective additives in the BCP robocasting procedure. Some additives are essential in ink preparation, while others could enhance the desirable features. The final physical and biological performance of the fabricated scaffolds depends mainly on the prepared ink and its properties.

Green body scaffold fabricating

Green body is a term dedicated to the scaffolds that are not condensed by heating procedure after printing [144]. Green body scaffold fabricating is possible via AM techniques, especially robocasting. Even though the AM techniques, especially robocasting, are promising methods for fabrication of green body scaffolds, success in the engineering of complicated structures by AM is strongly dependent on the viscosity and formidability of employed ink [145].

In the case of ceramic-based scaffolds, the ceramic structure should be post-sintered, after fabrication by the AM method, to have adequate strength and stability. The alternative possibility is also strengthening the ceramic-based scaffolds in other ways instead of sintering [146]. Some ceramics such as tri-calcium silicate (Ca_3SiO_5, C_3S) possess the ability to consolidate via soaking in the water; while utilizing photosensitive resins and UV sources are other methods [146,147].

Maeng *et al.* [148] studied green body scaffold manufacturing procedures using frozen terpene crystals. They claimed that BCP/ frozen terpene crystals composite surrounded by BCP/ urethane di-methacrylate (UDMA) walls can extrude through a fine nozzle and then effectively photo-polymerized by UV light. In this way, green filaments with high shape maintaining ability were prepared. Removing terpene crystals via freeze-drying method leads to producing some pores in BCP filaments, which were adjustable by modifying terpene content [148].

Ink preparation

A proper ink for robocasting is composed of binders and, in some cases, lubricant to flow from the storage under applied forces [149]. Based on previous studies, a composition of PVA and phosphoric acid could be used as binders to make biocompatible artificial stents with adequate compressive strength [149,150]. Some studies showed that using phosphoric acid as a binder has better performance on the mechanical properties of final printed BCP structure than PVA binder [149,150]; therefore researchers utilized it more than other materials in the ink preparation process [18,151-153]. Conversely, printed BCP structure by PVA binder have a higher absorbance rate and higher cell proliferation than the ones printed by phosphoric acids; therefore, choosing an appropriate binder composition plays a vital role in the robocasting process [150]. Furthermore, to achieve an acceptable viscosity of the ink in the robocasting, adding 0.25 wt% Tween80 to the binder solution is preferred [150].

Considering a specified amount of PEG as a lubricant for ink preparation as well as using poly-vinyl-pyrrolidone as a binder has attracted a lot of attention, in recent years [154]. Seitz *et al.* [154] employed 2 wt% dispersant lubricant to provide low viscosity slurry for using in robocasting and 4 wt% binder for preparing an appropriate slurry. Fig. 4b shows ink preparation-needed materials and efficient additives for BCP robocasting.

Efficient additives

All the materials that improve a specific feature of the ink and scaffold, are summarized as efficient additives. Materials that improve mechanical properties, adjust the ink viscosity and rheology, reduce the grain size, etc., are introduced as efficient additives. To manufacture the scaffolds with complicated structures, an admitted printing method, which uses sacrificial materials, is suggested [155]. Sacrificial materials act as supporting structures in the printing process, at the first, and should be removed after printing [156]. Pluronic® F-127 (BASF Corporation, USA) is a salient example of these materials commonly used in BCP robocasting for the temporary support [157]. Also, it can be used as an appropriate ink flow rate adjuster. Pluronic® F-127 content and its particle size in the ceramic powder are adjustable since they are influential on the flow of robocasting ink. It has been confirmed that the ink flow rate increases with the rise of Pluronic® F-127 content [157].

To improve the mechanical properties of BCP scaffolds, ZrO_2 has been proposed as an appropriate additive [65]. Woo *et al.* [65] added 10 wt% ZrO_2 to produce some BCP scaffolds, which led to better mechanical strength and osteogenic differentiation ability. They reported that by adding this amount of ZrO_2, the highest efficacy could be obtained: the best viscosity of printing along with the ideal mechanical properties [65]. Also, they found that the differentiation of human mesenchymal stem cells (hMSCs) indicated an elevated expression of bone morphogenic protein 2 (BMP-2), cultured on zirconia involved samples, compared with the samples containing no additive.

Additionally, graphene nanoplatelets (GNPs)-reinforced BCP scaffolds were prepared by Zhao *et al.* [158] via the hot pressing procedure. They reported that measuring the maximum bending strength and fracture toughness in parallel to the hot pressing direction, resulted in about 55% and 76% higher amounts than monolithic BCP scaffold, respectively [158]. Also, Peroglio *et al.* [159] demonstrated that the infiltration of BCP scaffolds with PCL improves their mechanical properties via crack bridging by polymer fibrils.

Previous studies demonstrate that PVA [160], Phosphoric Acid [161], Polyvinylpyrrolidone [162], Sodium Alginate [163], and Methacrylate-based photosensitive resins [164] are some efficient additives that have been used as binder in BCP robocasting procedure. Moreover, Hydroxypropyl Methylcellulose (HPMC) and Polyethylenimine (PEI) [65] were used as ink flow rate adjuster and flocculant, respectively, to regulate the ink viscosity.

Adding Mg^{2+} to the BCP compound could significantly decrease grain size and increase density and mesoporous precipitates after sintering [165]. Ramezani *et al.* [166] added diopside ($MgCaSi_2O_6$) powders, which had approximately 30.0 ± 4 nm size, to the BCP scaffolds, which decreased the prepared scaffold's grain size. They reported that increasing the diopside powder content from 0 to 15 wt% resulted in a considerable drop in the scaffolds' average grain size from 6 ± 0.9 μm to 1.9 ± 0.6 μm, respectively [166]. Several studies showed that grain size significantly affected physical, mechanical, and biological characteristics [165,167]. An undeniable fact, which should be considered, is the additive's content and its amount. For example, the extra accumulation of Ca^{2+} ions in β-TCP scaffolds hurt the osteoblastic cells [168].

Robocasting of BCP

Robocasting of BCP-based scaffolds have been a matter of discussions and debates in developing 3D complicated scaffolds for BTE applications (Table 2). Franco *et al.* [157] worked on the fabrication of the Calcium Phosphate scaffolds using the robocasting and ceramic powders involved- Pluronic® F-127 solution inks. They developed HA, β-TCP, and BCP with the HA: β-TCP ratio of 35: 65. Pluronic® F-127 acts as a non-ionic block copolymer that does not affect the slurry's pH value. They reported that decreasing the sintering temperature as well as increasing the amount of Pluronic® content led to an increase in the scaffold micro-porosity. They also observed that increasing the amount of micro-porosity was an essential feature of biological response but has a direct negative effect on the scaffold strength. Also, by measuring the shrinkage of the produced specimens, they found that the shrinkage rate was not the same in different directions.

Petit *et al.* [169] made BCP scaffolds containing 80 wt% HA and 20 wt% β-TCP via the robocasting method. They intentionally added poly-methacrylate (PMMA) beads to the compound to create artificial defects to investigate the impact of defects on the applied external stresses in uniaxial compression experiments. By observing specimens with structural defects over compressive loading, it can be concluded that control of defect formation can remarkably prevent the initiation of cracking and propagation. *Ex-situ* experiment's results showed the brittle behavior of the specimens due to the presence of defects and crack initiation in the sample [169]. Using finite element modeling (FEM), samples with existing artificial defects showed similar results to the struts' real condition. The findings showed that increasing the number of loading and unloading cycles leads to increasing the Young's Modulus in scaffolds.

Richard *et al.* [170] compared the mechanical properties and biocompatibility of two series of 3D printed scaffolds. In their work, cylindrical-shaped β-TCP and 50 wt% HA-50 wt% β-TCP scaffolds were fabricated by robocasting method. The average compressive strength of β-TCP and BCP samples were measured to be 11 ± 5.4 and 15 ± 6.9 MPa, respectively [170], which showed no significant difference. The results showed that 50 wt% HA-50 wt% β-TCP scaffolds, fabricated by robocasting methods, have more mechanical properties similarities to the natural bone than pure β-TCP scaffolds. They noted that the pore size and empty spaces in BCP scaffolds are more similar to the ingrowing trabecular bone, due to the metabolic activities such as vascularization, oxygen delivery, growth factors, and cell nutrition [170].

Seitz *et al.* [154] used HA, β-TCP, and BCP (with the composition of 60 HA: 40 β-TCP) for 3D printing. Various CaPs ratios were examined, which were sintered at 1250 °C to reach adequate mechanical strength. All granulates were less than 100 μm in diameter, which had a significant effect on the slurry's viscosity. The results showed that the pore channel size (200–600 μm) was significantly different from the theoretical size (580–870 μm) due to the sintering and shrinkage of 3D printed constructs. They suggested that the theoretical and actual size difference could be compensated in the parameter designing in the CAD stage. The results of the compressive strength test also showed that BCP and HA specimens had the highest and the lowest amount of compressive strength, respectively. Their findings also showed that there is a relation between the mechanical strength and the internal channel network. They concluded that diverse phase compositions of Calcium Phosphate (in the forms of HA, β-TCP, or BCP) could be employed in BTE applications that can adapt to their degradation behavior and mechanical properties.

Zhou *et al.* [165] used BCP nano-sized particles to regenerate the damaged bone tissue. By preparing precursors in the form of amorphous nanoparticles and then sintering at 900C, the dense BCP ceramic powders were obtained. They found that adding Mg^{2+} to the BCP powders increased the formation of β-TCP instead of β-Calcium Pyrophosphate (β-CPP). Their results also showed that decreasing the particle size, enhancing the density of the sintered ceramics, and strengthening the negative electric charge on the BCP surface have important roles in mechanical strength and cell proliferation. They also illustrated that the obtained precipitates are highly porous, composed of nanoscale and equiaxed particles, and can support vascularization and the formation of bone tissue and osteoblast cells. Due to mentioned properties and a high rate of similarity with natural bone features, their developed nano-sized particles can be extensively 3D printed and used as bone grafts.

Castilho *et al.* [63] studied the synthesis and fabrication of HA/β-TCP/Calcium Carbonate bone scaffolds using Phosphoric Acid as a binder on a hydraulic setting reaction of a binder/powder. They employed an extrusion-based 3D printing method to develop complexly shaped BTE scaffolds, using the starting powders for the

Table 2
Summary of BCP-based bone scaffold robocasting studies representing the biomaterials, compressive strength, additional elements, and porosity size.

Biphasic materials	Compressive strength of BCP (MPa)	BCP weight ratio (HA: β-TCP)	Compressive strength of HA: β-TCP (MPa)	Additional elements on scaffolds	Cell type / source	Pore size (μm)	Ref.
HA/β-TCP	34	35: 65	102: 77	Pluronic® F-127 solution	–	200 μm between lines and a layer height of 180 μm	[157]
HA/β-TCP	14.2	80: 20	–	–	–	30–80	[169]
HA/β-TCP	15	50: 50	-: 11	Hydroxypropyl methylcellulose (HPMC)	–	500	[170]
HA/TCP	1.1	60: 40	0.7: 0.8	Polyvinylpyrrolidone, poly(ethylene glycol) (PEG)	–	100	[154]
HA/β-TCP	22	60: 40	–	calcium peroxide (CPO), polycaprolactone (PCL)	Human osteoblasts	500	[171]
HA/β-TCP	21	60: 40	–	CPO, PCL	Human osteoblasts	500	[172]
HA/β-TCP	23	60: 40	–	CPO, PCL	Human osteoblasts	500 and 300 in vertical direction	[173]
HA/β-TCP	2.6 (60/40)	100: 0, 20: 80, 40: 60, 60: 40	–	phosphoric acid, polyvinyl alcohol, Tween 80	Bone marrow / New Zealand rabbits	800	[150]
Calcium pyrophosphate (CPP)/β-TCP	–	–	–	Mg^{2+}	MC3T3-E1 osteoblastic cells	–	[165]
HA/β-TCP /Calcium carbonate	1.81	30: 70	–	PLGA solution as a coating layer	osteoblastic cell line MG63	300	[63]
HA/β-TCP	4.32	–	–	SI500 photocurable liquid polymer resin	NIH3T3 cells, dental pulp mesenchyme from the mandibular incisor of P3.5 mice	–	[174]
HA/β-TCP	1.23	60: 40	–	Methacrylate	–	–	[175]
HA/β-TCP/ Chitosan	–, 1.5, 2	23: 77, 46: 54, 87: 13	–	Chitosan, genipin	human dermal neonatal fibroblasts	500	[176]
HA/β-TCP	11	–	–	ammonium polycarbonate, HPMC, and polyethylenimine	human osteosarcoma derived MG-63 cell line	120–500	[177]
HA/β-TCP/PVA	0.4	60: 40	–	polyvinyl alcohol (PVA), Platelet-rich fibrin (PRF)	bone marrow-derived mesenchymal stem cells (BMSCs) / male New Zealand White rabbits	500–600	[178]
HA/β-TCP	–	60: 40	–	2 wt% dispersant (acrylic acid copolymer)	Monocytic cells from the RAW 264.7 cell line	100	[179]
HA/β-TCP	–	35: 45	51: 15	Darvan® C dispersant, HPMC, and PEI	–	250	[180]

printing process, consisted of β-TCP and Calcium Carbonate mixtures in different Ca: P ratios of 1.65, 1.71, 1.83, and 2.00. Upon printing the specimens, they were sintered at 1200̊C for 5, 10, and 15 h to induce a partial phase transition from the mixture of β-TCP and Calcium Carbonate into HA. The final HA amount in the printed specimens was depended on the molar ratio of β-TCP to Calcium Carbonate at the start point. The authors confirmed that the compressive strength of the BCP scaffold is directly related to the amount of β-TCP. However, the micro-porosity in the scaffold was entirely independent of the BCP compounds. The results also showed the highest cell proliferation and growth in BCP scaffolds compared to either HA or β-TCP scaffolds. Their findings also showed that increasing the Ca: P ratio caused increasing the toughness modulus of fabricated scaffolds. They also claimed that increasing the amount of porosities and decreasing the grain boundaries of the scaffolds led to decreasing the resistance of printed scaffolds to the crack propagation. The authors also confirmed the use of the robocasting method for fabricating BCP-based bone substitutes, based on mechanical properties, porous structure, pore size, and interconnectivity [63].

Fig. 5 shows the robocasted BCP scaffolds and their corresponding SEM images. As shown in this Figure, BCP constructs could be printed using nozzles in various diameters (Fig. 5a-c). However, using nozzles with small internal diameters lead to shrinkage of the distance of the rows and minify the porosities. The printed constructs possess ordered layers on each other that result in proper mechanical and biological performances (Fig. 5d). Fig. 5e-h show the optical view from BCP scaffolds produced by Touri *et al.* [172,173] along with the corner, top and cross-section SEM views. They reported that the distance among the printed rods and the diameter of each rod was approximately 500 μm. Miranda *et al.* [180] showed SEM images of HA, β-TCP, and BCP scaffolds, possessing a rod diameter of 220 μm as well as a 50 μm gap between rods (Fig. 5i-l). The further details of the grains' morphology are available in Fig. 5m-p [157].

Wang *et al.* [150] printed BCP scaffolds using two ink binders, including a combination of 0.6 wt% polyvinyl alcohol (PVA) + 0.2 5 wt% Tween80, and a combination of 8.75 wt% phosphoric acid + 0.25 wt% Tween80. The results showed that HA: β-TCP bioceramic scaffold with a weight ratio of 60: 40 had the highest mechanical strength and adaptability to the cell culture medium among all examined samples with different weight ratio of HA: β-TCP, including 20: 80, 40: 60, and 60: 40. The authors showed that the compressive strength of all examined scaffolds increased with increasing the HA content. Moreover, they revealed that the binding mechanism in PVA and Calcium Phosphate powder is a

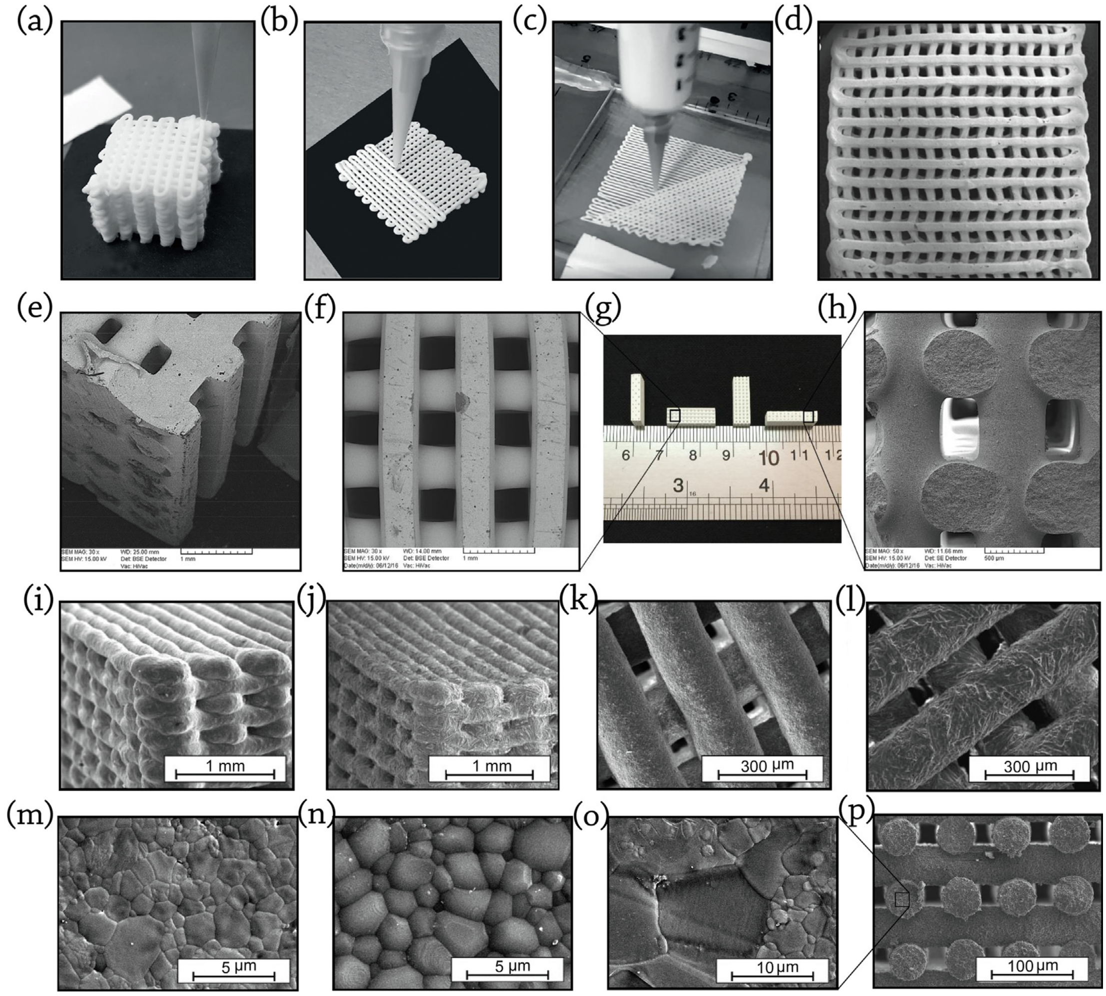

Fig. 5. 3D printed scaffolds using different nozzles in: (a) Ø 80 µm; (b) Ø 60 µm; and (c) Ø 40 µm, show that utilizing nozzles with small internal diameters lead to shrinkage of the distance of the rows and minify the porosities, reproduced with permission from [270] (d) The printed BCP/PVA scaffold having a high porosity and connectivity rate, reproduced with permission from [178] (e) SEM view from the corner of printed BCP scaffold, reproduced with permission from [172]. SEM images of the BCP printed scaffold from (f) top view (g) Optical view, (h) cross-section view, reproduced with permission from [173]. SEM micrographs showing the morphology of: (i) printing plane view of HA scaffolds (j) printing plane view of β-TCP scaffolds (k) detail of the HA rod surface (l) detail of the β-TCP rod surface after sintering at 1300C for 2 h, reproduced with permission from [180]. SEM image of the: (m) HA scaffold (n) β-TCP scaffold after polishing and thermal etching (2 h at 1000C) along with: (o, p) their combination output (BCP), reproduced with permission from [157]. The micro and macro structure of prepared scaffolds affects the mechanical and biological features.

physical bond, whereas the Phosphoric Acid and powder's binding mechanism is a dissolution-precipitation reaction [150].

Kindly note that higher printing speeds are generally preferred since they shorten the time it takes to construct a component and allow for more consistent flow. On the other hand, high printing speed impair tool path accuracy when changing direction and cause sharp edges to become rounded. Buj *et al.* [181] reported that the relationship between infill and speed is critical. In general, low infill with low-speed results in high roughness values; however, a distinct combination of trials with high infill and fast speed also results in high roughness [181]. Low infill paired with fast printing results in the lowest roughness values. Low infill suggests that less material must be deposited on each layer, yet fast printing speed decreases printing time, minimizing ink drying and promoting proper ceramic layer deposition.

Although decreasing the printing time, a high printing speed could alter the mechanical performance of the scaffold [182]. Upon enhancing the printing speed, the filaments could not deposit correctly on the bottom layers printed before, and the connection among the filament and its bottom layer decreased, which would be altered the mechanical performance and the porosity amount of the fabricated construct [182]. Therefore, increasing the extruding velocity is suitable only if the connection and interaction between the layers could be constant. This could be achieved by enhancing the filling rate by increasing the material depositing pressure. Once again, it is emphasized that the optimum condition of each robocasting procedure should be driven, depending on the material and machine used.

An irrefutable issue in tissue engineering is tissue hypoxia, while the vascularization network is being formed. Hypoxia can diminish tissue regeneration via limiting the nutrients delivery, such as oxygen and glucose, as well as wastes removal [183]. Although utilizing additive manufacturing techniques could manage this challenge in various tissues' engineering, this issue still remains as a significant concern in engineered bone constructs. Therefore, researchers try to address this matter via novel ideas.

Touri *et al.* [171] demonstrated that bone tissue scaffolds equipped with Oxygen-generating elements/compounds could increase Oxygen concentration and cell survivability in around the 3D printed scaffolds. They developed 3D printed 60 HA: 40 β-TCP scaffolds coated by Calcium Peroxide-included Polycaprolactone (PCL) [171]. PCL was used in scaffold coatings to reduce Calcium Peroxide (CaO_2, CPO)'s Oxygen release rate and prevent a burst release. Their findings showed that the samples with 3 wt% CPO in the coated layer had a high potential ability to enhance Osteoblast cell viability and improve bone tissue regeneration. Their research depicted that the use of Oxygen-generating elements, such as CPO in developing BTE scaffolds could affect cell viability, differentiation, and proliferation.

The osteoblastic function was monitored by measuring the amount of Alkaline Phosphatase (ALP) activity, which is a good criterion for measuring Osteoblasts' differentiation and mineralization. Results showed that scaffolds containing 3 and 5 wt% CPO had better ALP activity than other samples. They also concluded that CPO-included PCL-coated scaffolds had a high potential for bone formation [172]. In the next step, developed scaffolds were implanted in a rabbit's radius bone to evaluate the bone growth and healing process *in-vivo*. Based on previous studies, at least Oxygen release with the pressure of 25 mm Hg is required for cell proliferation and differentiation in most tissues [172,184]. Finally, by decreasing the number of live cells through increasing the content of CPO, the safety of developed scaffolds containing 3 wt% CPO was concluded [172,184].

Schumacher *et al.* [185] studied the effect of different weight ratios of materials used in the process of BCP preparation on the mechanical properties and porosity of final scaffolds. They worked on the shape and angle of the pores in prepared scaffolds by ink-jet printing to investigate their effect on compressive strength. Fabricated BCP composites consisted of HA: β-TCP with weight ratios of 80: 20, 60: 40, 40: 60, and 20: 80, were studied in different pore patterns [185]. They concluded that the composition and microporosity of printed BCP scaffolds had a significant effect on the compressive strength. The maximum compressive strength was reported up to 27.6 MPa for the printed scaffold with round-shaped pores, where the composition with 60/40 ratio of HA: β-TCP, possesses 26.0 % volume porosity. As they reported, the experiments' observations show a decrease in the compressive strength of the scaffolds by increasing the porosity volume. They conducted their research on the statically & dynamically cell culture effects on three types of the printed scaffold: pure HA, BCP with the composition of 60 wt% HA: 40 wt% β-TCP, and pure β-TCP [168]. The results of ST-2 bone marrow stromal cells (BMSCs) culturing on the scaffolds showed that the cell proliferation and growth rate in the dynamic culture condition were far better than the static one; this can be due to the accumulation of waste and shortage of nutrients inside the scaffold in the static culture, while the culture medium perfusion in dynamic situation compensate it [168]. Beside the fact that almost all studies have shown that BCP is a suitable bone substitute that can accelerate the bone regeneration process [174,186], its performance *in-vitro* and *in-vivo* should be more discussed.

In-vitro evaluation of BCP scaffolds

Detsch *et al.* [187] performed an *in-vitro* study of osteoclastic cell differentiation on 3D printed Calcium Phosphate bone scaffolds, including pure HA, pure β-TCP, and BCP, possessing a composition of 60 wt% HA: 40 wt% β-TCP. They investigated the osteoclastic cells' activation, proliferation, and differentiation using monocytic cell line RAW 264.7, and demonstrated that Osteoclast-like cells could adsorb on the surface of scaffold containing Calcium Phosphate granules. The authors showed that 3D printed BCP scaffolds had the best performance for Osteoclast activation. As Osteoclasts express highly tartrate-resistant acid phosphatase (TRAP, especially isoform 5b) [187], the TRAP staining is used commonly to distinguish between TRAP-positive Osteoclasts and undifferentiated monocytes. Their results depicted the monocytic precursor cells' differentiation into Osteoclast-like cells in 21 days of culture, while TRAP-positive cells were observed on all samples.

Detsch *et al.* [187] also evaluated lacunae formation on the scaffolds' surface upon the cells' removal from the scaffolds after 21 days. Lacunae's diameter and depth could be determined via a 3D model generated from three SEM stereo images using specialized software (MeX 5.0; Alicona Imaging, Austria). They reported that apparent differences in lacunae formation could be found, depending on the scaffold's surface material. HA surface led to only acidifications and sporadic lacunae, while the β-TCP scaffold's surface showed no osteoclastic resorption. Meanwhile, the BCP scaffold witnessed many lacunae on its granules. Moreover, the highest rate of resorption lacunae was observed on the BCP scaffold, with the HA: β-TCP composition rate of 40: 60 [187].

Yang *et al.* [75] evaluated the degree of *in-vitro* bioactivity of GENESIS-BCP™ and MBCP®, which is extended throughout for up to four weeks. They found that the former maintains bioactivity throughout, while the latter is only partially activated over four weeks. Also, they noted that GENESIS-BCP™ possess a superior bioactivity degree in comparison with MBCP® bone graft [75].

Hosseinabadi *et al.* [188] evaluated the yield strength and the elastic modulus of PLGA and PLGA/BCP composite scaffolds before and during *in-vitro* degradation. For this purpose, they used nanogranules of BCP, with various compositions, between 10 and 50 wt % as a reinforcing material. All samples were fabricated by the TIPS method, possessing more than 89% porosity. Their study showed that PLGA/BCP scaffolds have better mechanical properties and more weight loss than pure PLGA during eight weeks of *in-vitro* degradation. They noted that adding 30 wt% BCP cause the highest yield strength among other samples during the first six weeks of *in-vitro* degradation [188]. Also, they emphasized that decreasing the pH value arising from the acidic degradation products of PLGA could cause cell death. Besides, the released Alkaline ions during the degradation period, emitted from the BCP nano granules, could prevent the creation of the acidic environment. They noted that increasing BCP particles in the composite scaffolds results in increasing the hydrophilicity, which led to more weight loss. At the same time, the degradation rate of the PLGA polymer in the composite scaffolds was decreased by the presence of Alkaline ions [188].

Nie *et al.* [189] developed scaffolds based on a composition of BCP/PVA through the emulsion foam freeze-drying method. They indicated that the pore size, strength, and porosity of the scaffolds could be controlled by optimizing the BCP/PVA weight rate, while they fabricated composite scaffolds possessing 20, 30, 40, and 50 wt% PVA. Moreover, *in-vitro* degradation and cytocompatibility of scaffolds investigated a low variation of pH values (approximately 7.18–7.36) in the SBF solution. Increasing PVA concentration leads to a decrease in the degradation rate of BCP/PVA scaffolds. Their study on MTT assay indicated that the BCP/PVA porous scaffold has no negative effect on cell growth and proliferation, and the human bone mesenchymal stem cells (hBMSCs) possessed a convenient spreading morphology on the BCP/PVA scaffold surface.

In-vivo evaluation of BCP scaffolds

Ventura *et al.* [98] aimed to evaluate the bone regeneration capability of BCP powder-loaded Porcine dermis decellularized ECM composite. They fabricated two types of injectable composites, containing 10% and 15% w/v BCP in ECM hydrogel (Fig. 6a and b). Then, they implanted prepared hydrogels in the rat femoral head for an assessment of four and eight weeks. Based on their micro-CT and histological staining results, the fabricated injectable BCP–loaded decellularized ECM hydrogels illustrated an elevated bone formation compared with the unfilled defect (Fig. 6c). A nota-

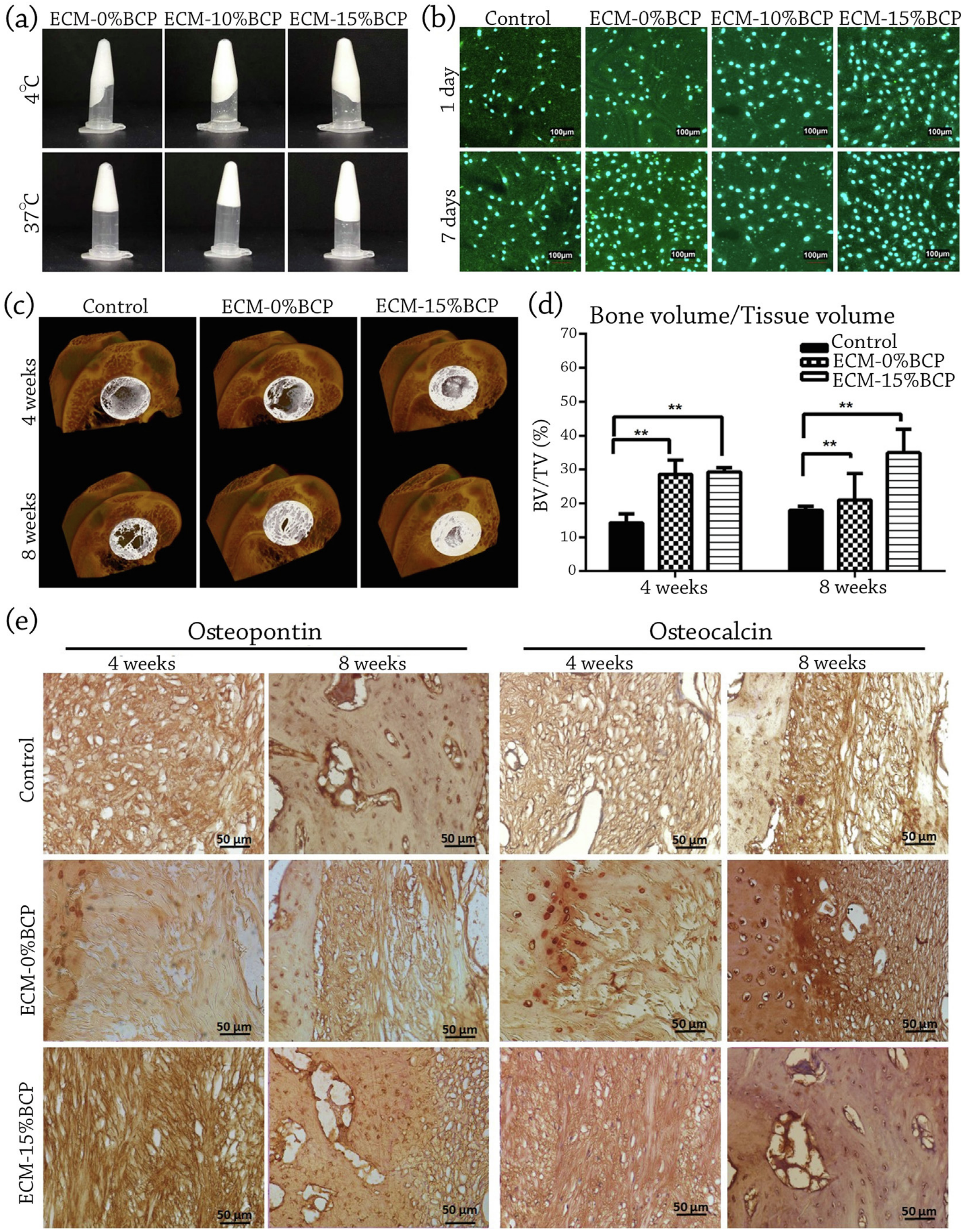

Fig. 6. (a) The gelation and preparation of Porcine dermis decellularized ECM containing different content of BCP (b) Confocal micrographs showed that the injectable ECM hydrogel extracts do not affect the morphology and proliferation of MC3T3-E1 cells after 24 h exposure. (c) Representative sample of 3D reconstructed Micro-CT of the femoral head explant with white color as the defect site of control (d) Bone volume/tissue volume quantification showed significant increase in bone formation ability of ECM-15 %BCP implanted in rabbit's femoral head defect after four and eight weeks (**$p < 0.005$ denotes significant difference) (e) Representative sample of high magnification of positive stain of Osteopontin and Osteocalcin of the central defect of the representative sample of control, ECM-0% and ECM-15 wt% BCP implanted in femoral head after four and eight weeks. (Scale bar = 50 μm), (a-e) reproduced with permission from [98]. Bone formation in eight weeks witnessed a 1.165 and 1.941-fold increase in ECM alone injected, and the defect with ECM-15 wt% BCP, respectively. At the same time, Osteopontin and Osteocalcin positive staining results approve this data.

ble progress has been seen in bone formation via ECM-15 wt% BCP in rabbit's femoral head defect after four and eight weeks through bone volume/tissue volume quantification (Fig. 6d). They concluded that developed injectable hydrogel possesses a high ability in non-load bearing BTE applications. The authors also reported that new bone formation in the defect filled with ECM alone and ECM-15 wt% BCP after four weeks injection was observed to be up-raised level of 2.00 and 2.055 fold compared to the unfilled control defect, respectively [98]. They also studied the bone formation in eight weeks and revealed that bone formation witnessed a 1.165 and 1.941-fold increase in ECM alone injected, and the defect with ECM-15 wt% BCP, respectively. Their claims positively correlates with Osteopontin and Osteocalcin positive staining results (Fig. 6e) [98]. Their study showed that the presence of BCP powder in Porcine dermis decellularized ECM composite could improve the osteogenic ability. As increasing the BCP amount from 0 to 15 wt%

Table 3
Pre-clinical and clinical studies performed on BCP scaffolds' evaluation.

Study type	BCP scaffold type	Model/site	Post-implantation study time	Primary outputs	Ref.
Pre-clinical (*In-vivo*)	10 and 15 wt% BCP powder-loaded Porcine dermis decellularized ECM composite	Rat femoral head	4 and 8 weeks	The fabricated injectable BCP–loaded decellularized ECM hydrogels showed an elevated bone formation compared with the unfilled defect	[98]
	GENESIS-BCP™ and MBCP® powder BCPs	10 mm bone defects in Mouse skull and damaged cortical sites of New Zealand white Rabbits	6, 12, and 16 weeks	They noticed that bone scaffolds based on GENESIS-BCP™ are well-established candidates for bone regeneration.	[75]
	MBCP®, and MBCP+® powder BCPs	Dorsum of the SWISS nude mice	–	MBCP® and MBCP+® scaffolds provided osteoinduced bone approximately 0.15% and 1.3% of biomaterial surface, respectively, without using any cells.	[71]
	100% HA, 100% β-TCP, and BCP with HA: β-TCP ratio of 76: 24, 63: 37, and 56: 44, 20: 80.	Mouse ectopic model	–	HA: β-TCP composition ratio of 20: 80 showed the fastest rate of bone induction	[190]
	Porous BCP scaffolds fabricated via robocasting, containing 3 wt% CPO and coated by PCL	Radius bone of a rabbit	–	Results showed that prepared bone constructs were suitable for apatite precipitation and bone ingrowth.	[172]
	Robocasted BCP/PVA bone scaffolds containing platelet-rich fibrin (PRF), using nano-BCP powder with a composition ratio of 60% HA and 40% β-TCP	Mouse ectopic model	4, 8, and 12 weeks	The printed BCP/PVA/PRF scaffolds released significantly higher levels of primary growth factors in the early stages than the non-printed BCP/PVA/PRF scaffolds. The presence of PRF in BCP/PVA bone scaffolds led to a better cell adhesion, proliferation, and osteogenic differentiation. BCP/PVA/PRF scaffolds showed better bone formation performance compared with BCP/PVA scaffolds.	[178]
Clinical	3D-printed BCP construct with a 30 HA: 70 β-TCP composition ratio	Human maxillary buccal plate	7 years	Biomaterial volume reduced by more than 23% and that newly produced bone volume constituted more than 57% of the entire mineralized tissue after 7 years of post-implantation. perfect scaffold integration, in which the soft tissue, biomaterials, bone portions were 15.2, 25.6, and 59.2, respectively.	[191]
	Various composition ratios of HA: β-TCP in the BCP scaffolds	Human fresh dental sockets	3 and 6 months	The newly formed bone in the alveolar defect area filled with HA: β-TCP scaffolds with the composition of 60.28: 39.72 and 78.21: 21.79 was reported to be 69.3% ± 6.03% and 46.6% ± 7.66%, respectively.	[192]

resulted in superior bone formation in eight weeks, it could be noted that used scaffold's composition and its structure possesses a vital role on osteogenesis.

Table 3 summerizes pre-clinical and clinical studies performed on BCP scaffolds' evaluation. As seen in this table, Yang *et al.* [75] investigated the GENESIS-BCP™ and MBCP® scaffold's efficacy implanted in the bone defects of mouse and rabbit samples. They implanted scaffolds into 10 mm bone defects in mouse skull and damaged cortical sites of New Zealand white rabbits and studied the new bone formation at 6, 12, and 16 weeks post-implantation. The authors prepared Hematoxylin and Eosin (H&E) stains and micro-CT images to evaluate the amount of newly bone formation. They found that GENESIS-BCP™ scaffolds are more efficient in bone formation in mouse skull compared to the MBCP® scaffolds. In the case of rabbits, the authors concluded that both scaffolds were efficient in bone formation performance, while GENESIS-BCP™ scaffolds showed more appealing results than MBCP®. They noticed that bone scaffolds based on GENESIS-BCP™ are well-established candidates for bone regeneration.

Miramond *et al.* [71] performed an *in-vivo* study to investigate the osteoinductivity of two available commercial BCP in the market, MBCP®, and MBCP+® through forming several pockets of implantation on the dorsum of the SWISS nude mice. MBCP® and MBCP+® scaffolds provided osteoinduced bone approximately 0.15% and 1.3% of biomaterial surface, respectively, without using any cells. They reported a high similarity of physicochemical characteristics among two mentioned scaffolds. Their study showed that MBCP+® scaffold possesses a higher ionic exchange rate with host tissues, while it has a higher *in-vivo* dissolution rate, too. The authors pointed out that the higher content of β-TCP could cause a difference in osteoinductivity.

Arinzeh *et al.* [190] carried out an examination to evaluate the suitable ratio of HA: β-TCP, promoting bone formation. Seeding hMSCs on BCP samples with HA: β-TCP composition ratio of 20: 80 showed the fastest rate of bone induction in a mouse ectopic model among all examined samples of 100% HA, 100% β-TCP, and HA: β-TCP ratio of 76: 24, 63: 37, 56: 44, and 20: 80 (Fig. 7a-f).

Touri *et al.* [172] proposed the implantation of porous BCP scaffolds fabricated via robocasting, containing 3 wt% CPO and coated by PCL in the radius bone of a rabbit model to evaluate the scaffolds' bone regeneration efficacy (Fig. 7g). They have shown that the oxygen released from prepared scaffolds caused an elevated rate of cell density, viability, and proliferation. They also claimed that prepared bone constructs were suitable for apatite precipitation and bone ingrowth.

Song *et al.* [178] developed robocasted BCP/PVA bone scaffolds containing platelet-rich fibrin (PRF), to investigate the effect of PVA and PRF on the bone regeneration capability. Also, to deter-

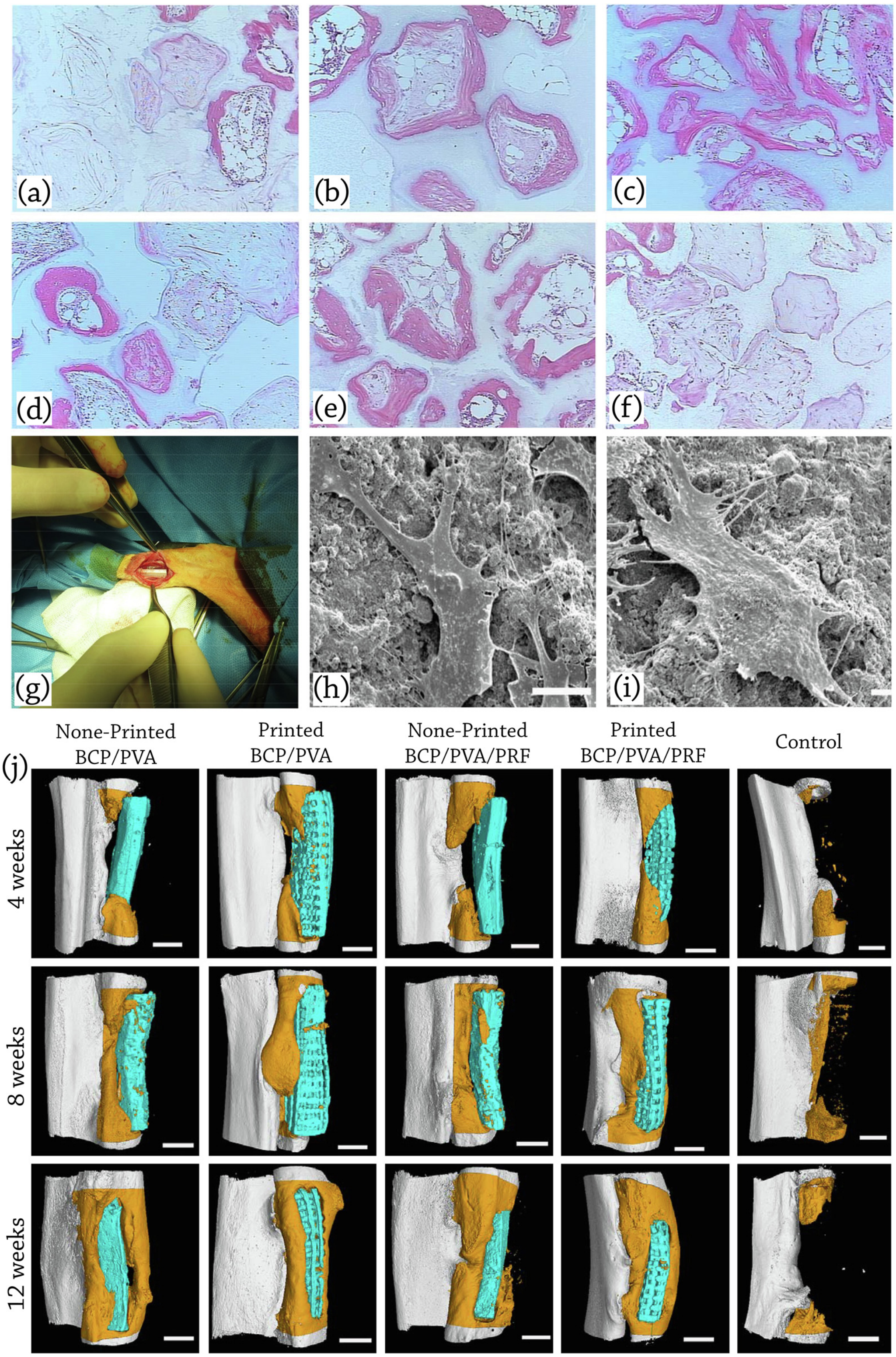

Fig. 7. *In-vivo* applications of BCP scaffolds: representative histological micrographs of (a) 100 HA, (b) 76 HA/24 β-TCP, (c) 63 HA/37 β-TCP, (d) 56 HA/44 β-TCP, (e) 20 HA/80 β-TCP, and (f) 100 β-TCP at 12 weeks post implantation (H&E staining). Bone is stained pink, ceramic has a shadowy white appearance, loose connective tissue is stained a light pink, cells are stained a dark pink, reproduced with permission from [190]. Seeding hMSCs on BCP samples with HA: β-TCP composition ratio of 20: 80 showed the fastest rate of bone induction in a mouse ectopic model among all examined samples. (g) Implanted scaffold in the radius defect of the rabbit; reproduced with permission from [172]. (h) SEM analysis of the adhesion status of BMSCs on the printed BCP/PVA scaffolds (i) printed BCP/PVA/PRF scaffolds, reproduced with permission from [178] (j) Micro-CT scans and 3D reconstructions to visualize healing of critical size bone defects in the rabbit radius at 4, 8, and 12 weeks after implantation of scaffolds seeded with BMSCs. Defects were implanted with non-printed BCP/PVA scaffolds, printed BCP/PVA scaffolds, non-printed BCP/PVA/PRF scaffolds, printed BCP/PVA/PRF scaffolds, and the sample with no following treatment (control). The scaffolds are shown in blue, and newly formed radius bone is shown in dark orange in the micro-CT images; scale bars: 3 mm, reproduced with permission from [178]. The incorporation of PRF, promoted the biological activity through enabling the sustained release of bioactive factors from the scaffold.

mine the preparing method's effect on scaffold's performance, they fabricated non-printed BCP/PVA scaffolds with/without PRF via freeze-drying technique, while they used nano-BCP powder with a composition ratio of 60% HA and 40% β-TCP.

The authors pointed out that the incorporation of PRF, promoted the biological activity through enabling the sustained release of bioactive factors from the scaffold [178]. They measured the GFs' concentration released from BCP/PVA/PRF scaffolds using enzyme-linked immunosorbent assay (ELISA) kits and reported that vascular endothelial growth factor (VEGF), platelet-derived growth factor-AB (PDGF-AB), transforming growth factor- β1 (TGF-β1), and insulin-like growth factor-1 (IGF-1) are the primary GFs assessed by ELISA. The printed BCP/PVA/PRF scaffolds released significantly higher levels of mentioned growth factors in the early stages and considerably lower levels at 14 and 21 days than the non-printed BCP/PVA/PRF scaffolds.

PRF is a fibrin matrix with a simplified preparation method, which does not require any Thrombin or Calcium Chloride addition [193]. In PRF, platelet cytokines and GFs are trapped, which are efficient in facilitating the hemostasis, wound healing, and the differentiation of pre-osteoblasts due to the presence of secreted GFs [194,195]. A variety of activated platelets and leukocyte GFs are involved in the fibrin matrix of PRF, while they could release gradually by degrading the fibrin [196]. Previous studies confirmed that PRF promotes Osteoblast adhesion, along with upregulating the collagen protein expression, which are almost effective in new bone formation [197-199].

As shown in Fig. 7h and 7i, the presence of PRF in BCP/PVA bone scaffolds led to a better cell adhesion, proliferation, and osteogenic differentiation. Also, *in-vivo* results after 4, 8, and 12 weeks implantation demonstrated that BCP/PVA/PRF scaffolds showed better bone formation performance compared with BCP/PVA scaffolds. In the term of the effect of fabricating method on the osteogenesis ability of developed scaffolds, 3D printed constructs showed better bone formation performance compared with freeze-dried ones (Fig. 7j), due to the fact that 3D printing generates an interconnected porous structure that is appropriate for cell survival and proliferation [200]. Existing adequate cell activity space, along with promoting its activity and proliferation via transferring the needed nutrients and oxygen to the cells and disposing of the waste materials, are fundamental merits of printed bone scaffolds compared with non-printed ones [201,202]. Extruded scaffolds have a precise, controlled internal architecture with programable interconnectivity, controllable porosity, and various structure, loading a variety of drugs and growth factors are possible. The drug and/or growth factor could be encapsulated in ink before the robocasting procedure or added following the extruding process prior to the cell seeding. Moreover, since mentioned advantages could accelerate delivering the drug, growth factor, and nutrients to the cells, the robocasted scaffolds could ameliorate the tissue growth and formation.

The biological responses of BCP

Chemical properties of bioceramics potentially affect osteoclast resorption activity. Ceramic solubility is undoubtedly among the most critical chemical features to regulate. It is irrelevant to assert that increasing the solubility of ceramic will optimize resorption activity. In contrast, manufacturing a ceramic that is excessively soluble may result in a significant gradient of calcium ions that is particularly detrimental to the activity of osteoclasts. Given that ceramic solubility is mainly determined by the HA: β-TCP ratio, various research sought to establish the optimum chosen ratio [28-30].

Yamada *et al.* [203] evaluated CaPs with varying degrees of solubility according to HA: β-TCP ratios [30]. Pure β-TCP and BCP with the composition ratio of 25 HA: 75 β-TCP showed resorption activity, while 75 HA: 25 β-TCP or pure HA did not resorb in osteoclasts. The authors discovered that solubility affects the pattern of osteoclastic resorption in terms of the form and distribution of resorption lacunae. Lacunae appear discontinuous on pure β-TCP, suggesting a chain of tiny islands, though they are huge and continuous on BCP with the composition ratio of HA/β-TCP (25/75), matching those on bone. Furthermore, the transition from resorption to migration seems to occur quicker on β-TCP than on HA/β-TCP (25/75) sample.

Regarding ceramic degradation, some free ions are produced via solubility and resorption activity. Depending on the HA/β-TCP ratio, these free ions may exist in the surroundings of bone progenitor cells, which might therefore activate osteogenic differentiation, contributing to new bone formation. Osteoblasts, for instance, react immediately to changes in Ca^{2+} concentration in the bone microenvironment [204], and mesenchymal stem cell osteoblastic development is followed by developing Ca^{2+} binding proteins and Ca^{2+} incorporation into the ECM [205]. Furthermore, an increase in inorganic phosphate has been demonstrated to operate as a particular signal, influencing the expression of several genes involved in skeletal cell proliferation, differentiation, mineralization, and apoptosis [61]. Inorganic phosphate, more specifically, controls the expression of numerous mineralization-related genes, including osteopontin and matrix Gla protein (MGP) [35]. ALP also stimulates type I collagen mineralization by reducing the inhibitory impact of inorganic pyrophosphate ions on mineralization by hydrolyzing inorganic pyrophosphate ions into inorganic phosphate. A continuous release of inorganic phosphate was demonstrated to upregulate collagen mineralization by overcoming the inhibitory action of inorganic pyrophosphate ions. In a corollary, by adjusting the composition ratio of HA/β-TCP, it should be feasible to influence not only the resorption rate of BCPs, but also the release of ions near bone cells, and therefore alter the biological features of BCPs.

Microparticles emitted by CaPs may be lysed by the monocytic-macrophage lineage cells, resulting in an inflammatory reaction marked by cytokine production. Among them, tumor necrosis factor (TNF-α) is likely to encourage bone repair by inducing osteoprogenitor cell recruitment [206]. Remarkably, Lu *et al.* [207] proposed that this release was caused by the sintering process. It is commonly known that BCP substitutes must be sintered at 1160C. As a result, HA microparticles of BCP constructs are incompletely sintered and quickly released following immersion or implantation. They revealed that microparticles produced by BCP might cause local inflammation and cell damage, influencing osteogenesis [207]. Also, Fellah *et al.* [208] verified the negative inflammatory response caused by microparticles on osteogenesis.

Furthermore, Silva *et al.* [209] investigated the effect of BCP microparticles (particle size $\sim$ 37 μm) on human macrophage motility and secretion. They discovered that cells and BCP granules were connected to one another. Cells linked to BCP had a greater intracellular free Ca^{2+} concentration than non-attached neighbors and released CaP particles into the medium. The authors investigated that released particles had a Ca/P ratio of 1.64, which is comparable to HA [209]. These produced particles may form a transition zone that promotes further macrophage attachment.

It has also been shown that fibroblasts and osteoblasts effectively ingest particles that interfere with their biological processes. Finally, the response of hMSCs as osteoblast precursors to bioceramic particles may be critical for effective bone regeneration [210,211]. A few previous researches describe the effect of bigger BCP particle sizes on cell behavior. Cordonnier *et al.* [212] discovered that by seeding hMSCs on BCP microparticles (particle size $\sim$ 140–200 μm), cells adhered and proliferated more quickly in the initial days of culture compared to culture on plastic. Anal-

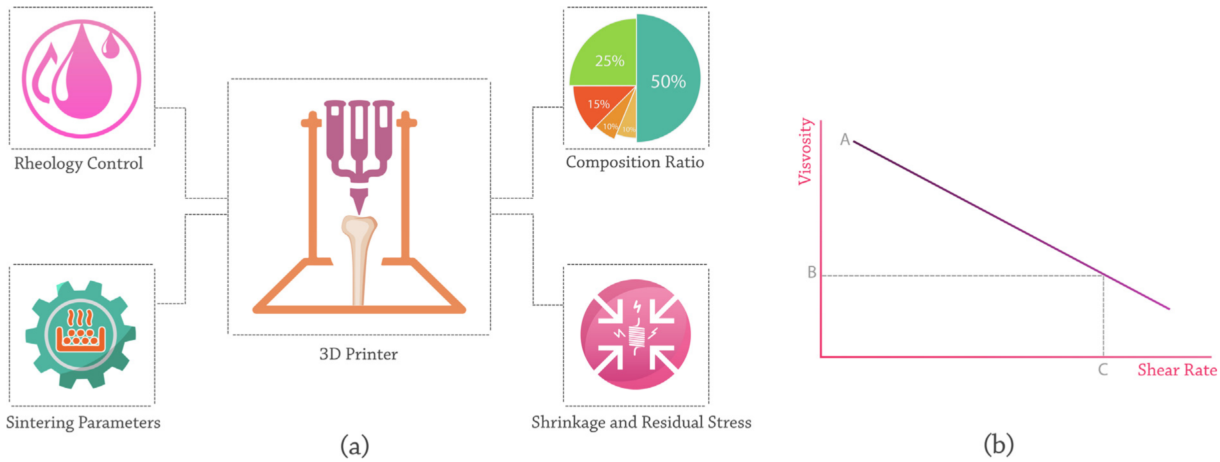

Fig. 8. (a) A schematic of BCP robocasting challenges (b) Shear-thinning behavior illustrating stages of the robocasting: A. rest and flow initiation, B. high shear rate in the nozzle tip walls, and C. wall shear rate.

yses of hMSCs cultivated on BCP particles without osteogenic factors demonstrated substantial ECM formation, resulting in 3D hMSCs/BCP particles constructions within a few days.

Challenges in BCP robocasting

As with any recent technology, BCP robocasting procedures also suffer from significant challenges, divided into the material- and machine-related issues. The majority of the problems, limitations, and drawbacks of the procedures are mainly related to the material properties' being printed. Machine-related challenges are discussed in the electrical and mechanical sections in previous studies [149,213]. However, material-related problems in BCP robocasting, including rheology control, composition ratio, sintering parameters, and shrinkage and residual stress will be discussed in the following sections (Fig. 8a).

Rheology control

Rheology is the science which considers the flow and deformation of soft materials and investigates the relationship between shear stress, shear strains and time [214]. An ink with appropriate rheological properties for robocasting should possess relatively low viscosity under stress. This means that the ink should be able to flow through the nozzle during the extrusion process which leads to formation of filaments instead of drops [215].

A paste-like material, prepared as robocasting ink can efficiently dispense through the nozzle tip at low viscosity, while it would lead to making spreads and collapses [215]. Besides, high viscosity causes difficulty dispensing along with requiring higher pressures. Therefore, the shear-thinning effect could be an ideal mechanism for robocasting applications.

Considering the shear-thinning behavior in colloidal dispersions, Fig. 8b illustrates the viscosity behavior versus shear rate. Low shear rates demand high viscosity, while low viscosity is desirable for high shear rates [214]. As the nozzle tips witness high shear rates in their walls, low viscosity could cause a better material deposition. The paste must possess an adequate shape retention capacity upon deposition and should tolerate high yield stress along with elastic modulus.

As molecules and particles of the ink are oriented in the flow direction throughout the shear process, increasing the oriented particles reduces flow resistance [216]. On the other hand, rheological properties of ink used in the robocasting process can be tuned by using the productive additives like Ethylene Glycol [217,218], nano-structure Silicate particles [219], and Pluronic [157]. Nevertheless, based on previous studies, the importance of rheology controlling in this field is commonly underestimated, and printability is generally analyzed only as a function of viscosity [220]. Therefore, a clear correlation between the rheological properties and process is lacking.

Composition ratio

Many researches have been carried out, in recent years, to develop the BCP scaffold as a proper substitute for bone tissue regeneration [168,185]. Using both HA and β-TCP simultaneously can improve the strength and cell growth and differentiation of scaffolds [221]. Therefore, choosing an appropriate composition of HA and β-TCP seems to be required [150]. One of the main BCP robocasting challenges could be considered as the composition ratio of HA and β-TCP that would ultimate to the maximum efficiency of biological and mechanical properties. Due to the reports mentioned above, increasing the HA content would lead to improving cell performance and decreasing the mechanical properties of developed 3D printed scaffolds [222].

On the other hand, raising the β-TCP amount leads to better physical properties similar to the natural bone tissue [223]. Hence, mixing the proper amount of HA and β-TCP is the first step in developing BCP scaffolds for BTE. However, increasing the Ca: P ratio in the composition of BCP constructs reduces the compressive strength due to increasing the porosities in the structure [63,223]. Increasing the Ca: P ratio results in enhancing the $CaCO_3$ amount in raw powder. Disaffiliation of $CaCO_3$ in HA conversion during sintering leads to increase the CaO content in the sintered samples, which causes an elevated CO_2 release and raising the porosity [63].

Researches show similar mechanical properties of BCP scaffolds containing 50% HA and pure β-TCP. Using bioactive BCPs in the robocasting process has increased the hopes of improving bone injuries healing [170]. Studies also showed that sintering process has the final effect on BCP's composition ratio. As shown in the study of Petit *et al.* [169], sintering process has changed the composition ratio of HA: β-TCP from 80: 20 to 84: 16.

However, it has been reported that the composition ratio of 60 HA: 40 β-TCP has an elevated effect on bone fracture regeneration [171-173]. The results reported by Wang *et al.* [150] and Arinzeh *et al.* [190] are in a parallel line with Richard *et al.* [170] and Seitz *et al.* [154], demonstrating that increasing the β-TCP amount in BCP composition up to 40 wt% results in higher mechanical performance, while greater bone induction and biological properties require a higher amount of β-TCP.

Sintering parameters

One of the main challenges in ceramic robocasting is the sintering process, which has a significant effect on the mechanical performance of final robocasted samples. This procedure could increase the compressive strength of the printed samples up to four times due to the phase transition in TCP, without changes in the chemical composition [63,169]. As mentioned previously, Castilho *et al.* [63] developed the robocasting process for fabrication of HA/TCP/Calcium Carbonate ($CaCO_3$, CC) bone scaffolds, containing the Ca: P ratios of 1.65, 1.71, 1.83, and 2.00. They reported that over 10 h of sintering at 1200C, there were no changes in the phase composition of fabricated scaffolds. Some artificial structural defects could be developed during the sintering process; large defects would remain unsintered, while tiny pores among the solid particles could be closed [169].

SEM images showed that an incomplete sintering procedure could cause the rods' macro-porosity with a size range of 2.6 ± 1.1 μm [169]. Some studies also showed that micro-porosities are emerged in a relatively low sintering temperature (1100C) due to the insufficient compressing during the sintering process [224,225].

Elevated temperatures would lead to the opposite results in ceramic samples' sintering process due to increasing the possibility of transformation of chemical composition [226]. Franco *et al.* [157] sintered compressed BCP, β-TCP, and HA ceramic scaffolds at 1085C, 1100C, and 1200C, while Touri *et al.* [171,172] preferred 1190C for BCP samples, since increasing the temperature of sintering process leads to the possibility of α-TCP formation instead of an increase in HA: β-TCP content. Some studies indicate that temperature variation can be employed in the sintering process to control the porosity in the printed layers [227-229]. Hence, choosing an appropriate sintering temperature profile and other parameters needs to be more investigated.

Shrinkage and residual stress

The granules' gluing by the binder fluid and the shrinkage during the sintering process are two phenomena occurring during the robocasting process of the ceramic scaffolds. They are the primary agents of differences in the real and theoretical dimensions [154]. Both shrinkages can be measured using optical analysis, followed by analyzing via softwares such as analySIS, Soft Imaging Systems Corp. [185]. After printing, shrinkage may cause curling of the upper layers of the scaffolds. Seitz *et al.* [154] reported that the amount of linear shrinkage of BCP scaffolds obtained by adding binder fluid was in the range of 5–7%. Also, the sintering linear shrinkage rate was reported to be 26% for β-TCP and 30–32% for BCP and HA specimens [154].

The dimensions of the HA and β-TCP scaffolds were also measured by Schumacher *et al.* [168,185] before and after the sintering process using graphical analyzing software and stereo microscope. The results showed that the shrinkage rate was 26.3% and 15.1% for HA and β-TCP samples, respectively [185]. They reported that the change in pore sizes after shrinkage is due to the various behavior of used materials [168]. Kindly note that the amount of shrinkage after the sintering process of printed samples is reproducible. Considering the percentage of the shrinkage during the design process by CAD, it could be compensated before robocasting [154]. Furthermore, different shrinkage amounts at various directions should be considered in the CAD calculations [157].

Numerous studies have shown the importance of crack propagation in the robocasting process [169]. To investigate the adverse effects of cracks on the mechanical strength of scaffolds, Petit *et al.* [169] added some intentional defects in the structures of HA and β-TCP scaffolds by adding PMMA beads. However, the results showed a higher compressive strength of β-TCP than HA due to a faster rate of the crack spreading in HA [185].

Increasing the porosity of scaffolds is another factor that can enhance the likelihood of crack propagation on the scaffold [230]. Besides, based on observations during the sintering process of scaffolds, some micro-cracks initiate to grow. They increase the probability of fracture failure and decrease the mechanical strength of the scaffold.

Cracks might be generated just after the printing procedure, which could compensate by incorporating some additives to prevent its propagation [231]. Segre *et al.* [231] studied the effect of tire rubber particles on crack propagation in cement pastes. They pointed out that rubber particles act as crack stabilizer and toughness enhancer, resulting in decreasing the brittleness and propagation context. Also, crack propagation during the sintering procedure at the oven could be prevented by adjusting the heat treatment profile [232].

Post-processing of fabricated scaffolds

Coating

One way to overcome the crack progression in the printed scaffolds is coating the surface by a suitable material [171]. Yunqing *et al.* [233] observed better mechanical properties of the scaffolds and particularly high resistance to crack propagation by coating the β-TCP scaffolds with PLGA hydrogel. Nie *et al.* [234] prepared the multiply HA/poly-L-Lactide (PLLA) nanocomposites coated BCP scaffolds for BTE applications. They reported that by increasing the coating layer thickness, the biodegradation rate and compressive strength were reduced and increased, respectively. The authors claimed that multiply coating has not any adverse effects on cell growth and proliferation. They proposed using the BCP scaffold coated by multilayer HA/PLLA nanocomposites as an appropriate bone substitute [234].

Meanwhile, Castilho *et al.* [63] demonstrated that PLGA formed a fibril structure in the scaffolds, which increased the Modulus of toughness by approximately four-fold and ultimate compressive strength up to eight-fold compared to the non-coated specimens. However, although a surface coating of scaffolds using PLGA could increase the mechanical properties of the BCP-based bone constructs, PLGA suffers from principle disadvantages such as decreasing cell adhesion and secretion of acidic substances during degradation, which should be cared [63]. Meanwhile, as mentioned previously, researchers used materials such as CPO as an Oxygen-generating agent to reduce the hypoxia condition around the tissue and enhance the delivery of Oxygen and needed nutrients, which would lead to improve cell viability, proliferation and vascularization on the scaffolds [171-173,235]. Studies showed that adding an appropriate content of CPO can be useful in the vascularization process and the Osteoblast cell proliferation (Fig. 9a and b) [172,173].

Touri *et al.* [173] investigated a simulation study of robocasted BCP bone scaffolds to predict mechanical performance in uncoated and coated scaffolds (Fig. 9c). They developed longitudinal and transversal rods in 500 μm diameter with a 500 μm gap between the printed rods to fabricate the BCP scaffolds. They showed that CPO-included PCL coating increases the compressive strength of scaffolds approximately 9.5%. They indicated that crack propagation mostly initiates in the perpendicular direction of the longitudinal rods (Fig. 9d and e) [173].

The authors pointed out that appropriately designing of gaps interval between rods on scaffolds, affects achieving the appropriate cell viability. These intervals could influence cell culture and could have an impressive effect on the cell proliferation and vascu-

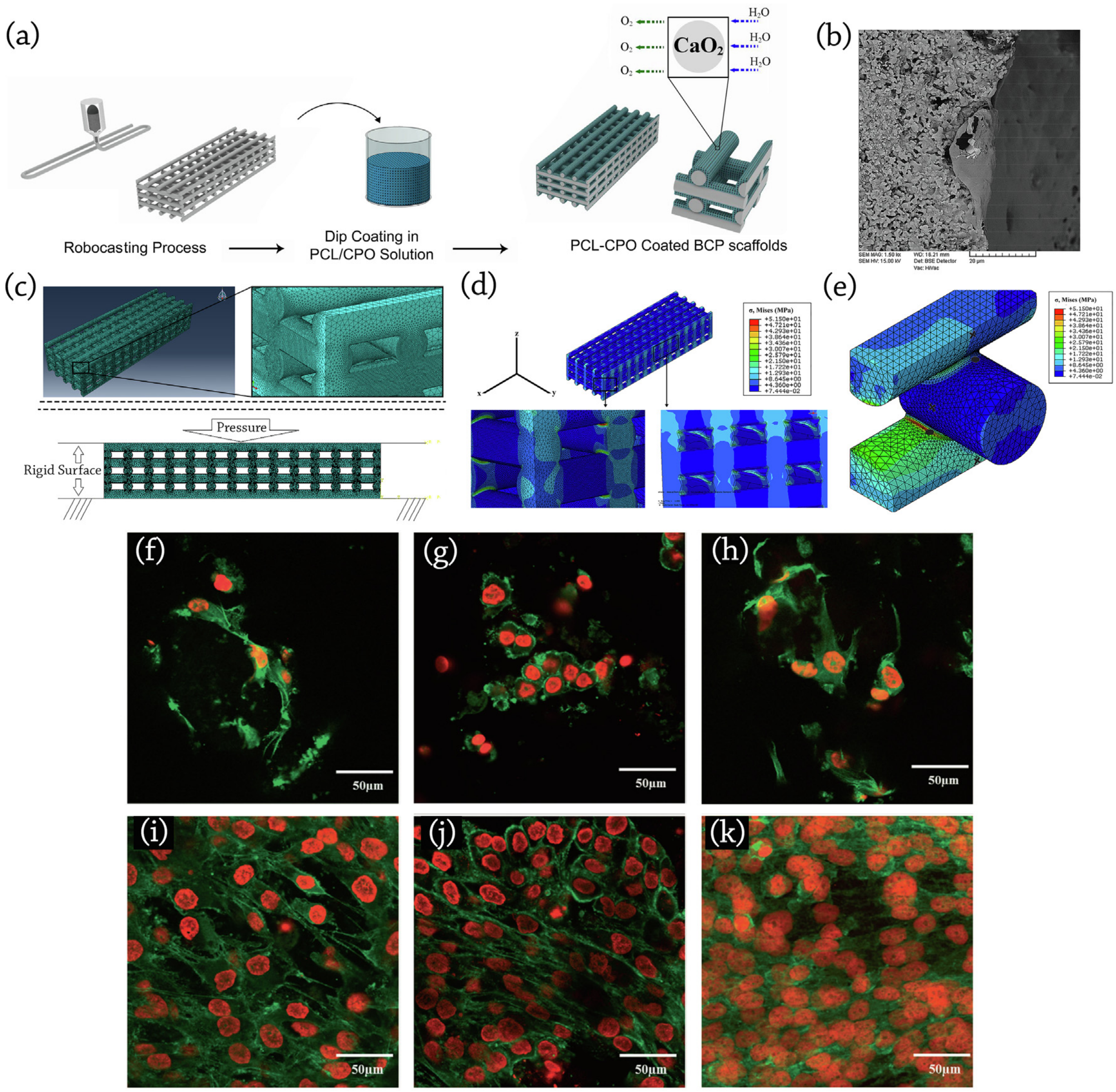

Fig. 9. (a) A schematics of CPO-included PCL-coated BCP 3D printed scaffolds and its fabricating procedure, reproduced with permission from [171] (b) A SEM image of CPO-included PCL-coated BCP scaffold shows the connection of coating layer on the BCP, reproduced with permission from [172]. Simulation of compression loading on fabricated BCP scaffolds: (c) Design and meshing the scaffold, and defining the load (d) Maximum stress results of the simulation over the whole scaffold (e) Maximum stress results of the simulation over the joints, reproduced with permission from [173]. Since a high amount of porosity in the scaffolds significantly reduces the compressive strength, rods' gap interval should be designed correctly to accomplish the consummate result, while using a coating layer could elevate the mechanical performance and cell attachment. Confocal images of cell adhesion behavior and growth morphology of MG63 cells on the surfaces of (f) non-coated BCP/ZrO_2 (g) BCP/ZrO_2 scaffold coated by PLGA: BCP with the weight ratio of 1:2 (h) BCP/ZrO_2 scaffold coated by PLGA: BCP with the weight ratio of 2:1 after 1 day of incubation; and (i) non-coated BCP/ZrO_2 (j) BCP/ZrO_2 scaffold coated by PLGA: BCP with the weight ratio of 1:2, (k) BCP/ZrO_2 scaffold coated by PLGA: BCP with the weight ratio of 2:1 after 7 day of incubation; reproduced with permission from [238]. PLGA coating promoted BCP/ZrO_2 scaffold's biocompatibility, cell adhesion behavior and cell growth.

larization. By the way, a high amount of porosity in the scaffolds significantly reduces the compressive strength. Hence, to accomplish the consummate result, rods' gap interval should be designed correctly, while using a coating layer could elevate the mechanical performance and cell attachment.

A polymer coating layer could reduce the brittleness of the ceramic scaffolds [236,237]. Many studies confirmed that ceramic scaffolds toughening via a polymeric coating is due to crack bridging by polymer fibrils [236,238,239]. Besides, polymer-coated scaffolds exhibit attractive properties in terms of controlled drug release; hence, the polymer-coated BCP scaffolds could be of interest in drug delivery applications to enhance bone regeneration [240]. Sadiasa *et al.* [238] developed a PLGA/BCP coating containing Simvastatin drug on BCP/ZrO_2 bone scaffolds to improve bioactivity performance (Fig. 9f-k). The developed PLGA: BCP composite coatings with the weight ratio of 1: 2, 1: 1, and 2: 1 showed improved biocompatibility and continued release of the Simvastatin drug. Moreover, enhancing the concentration of PLGA caused a reduction in porosity, degradation rate, scaffold's weight loss, and Simvastatin's release rate.

Simulated body fluid (SBF) soaking

Sample soaking in SBF stimulates mineral formation on the surface of bioactive scaffolds [241]. The similarity of the concentration of the ions in the SBF and human body plasma induces HA nucleation on the surface of soaked bioactive scaffolds [241]. The procedure is carried out via maintaining the pH and temperature of the solution in the vicinity of blood plasma characteristics [242]. Previous studies pointed out that the HA coating leads to better cell attachment and viability [243,244].

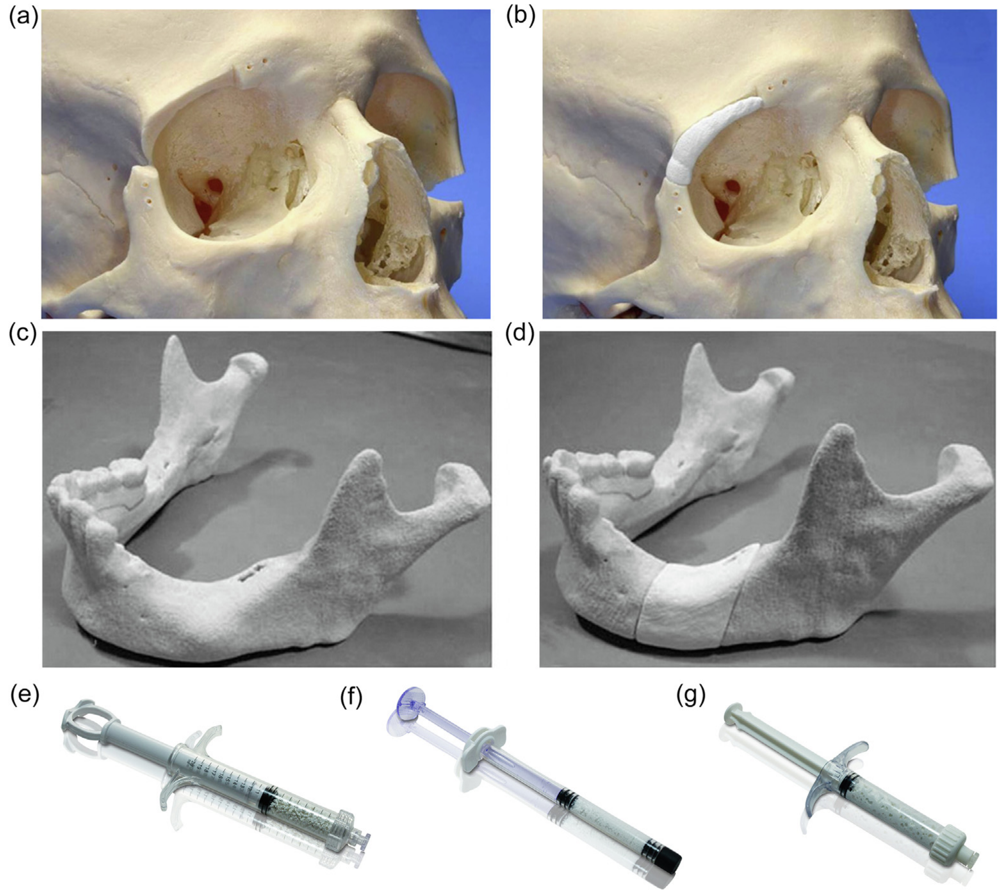

Fig. 10. Clinical application of Calcium Phosphate 3D Printed substances. (a) Skull with a defect in the orbital rim. (b) Printed and inserted BCP implant with an adequate accuracy of fit, reproduced with permission from [63]. (c) A model of human mandible with osseous tumor located on left body of mandible (d) Bone replacement of β-TCP adapted on the bone defect via a freeform 3D printed-scaffold for osseous defect, reproduced with permission from [271] (e) Commercial syringe MBCP® bone graft substitute (f, g) Commercial injectable BCP (In'Oss™) in two different cartridge sizes for clinical usage.

Immersing the BCP scaffolds in the SBF solution demonstrates that the amount of HA on the scaffold has increased [171-173]. In terms of CPO-coated scaffolds, it has been demonstrated that the highest amount of Apatite is formed on the surface of BCP scaffold containing CPO due to the gradual Oxygen releasing process, which helps in forming Osteoblasts [171]. SBF soaking procedure demonstrated an increase in the amount of Apatite precipitation on scaffolds and could be considered a valid post-processing proceeding, as it increases the viability and attachment of the cells cultured on the surface of 3D printed BCP scaffolds [171].

Clinical applications and future perspectives of BCP products

Although BCP scaffolds are the most often utilized bone substitutes in alveolar regeneration, BCP printed bone constructs have only been employed in a few clinical studies to date [192]. Even though a variety of methods in BCP scaffold fabrication have been utilized in clinical trials, there are a few studies to proceed with robocasted BCP scaffolds in the clinic. Mangano *et al.* [191] demonstrated in 2013, the patient underwent maxillary buccal plate bone regeneration using a 3D-printed BCP construct. They claimed that BCP grafted scaffold was embedded and integrated into the newly formed bone area, and due to the biocompatible and osteoconductive properties of BCP, it is possible to be used as a grafting material for Sinus Floor Augmentation.

After seven years, Mangano *et al.* [245] evaluated clinically and histologically the 3D printed BCP scaffold specimen with a 30 HA: 70 TCP composition ratio. A regenerated bone specimen was taken and processed for micro CT and histomorphometric analysis. The microarchitecture investigation using micro CT in the test-biopsy revealed that biomaterial volume reduced by more than 23% and that newly produced bone volume constituted more than 57% of the entire mineralized tissue. When compared to unloaded controls or *peri*-dental bone, the test sample seemed much more mineralized and bulky. Histological examination revealed perfect scaffold integration as well as evidence of particle degradation, in which the soft tissue, biomaterials, bone portions were 15.2, 25.6, and 59.2, respectively [245]. The authors investigated via polarized light microscopy that the biomaterial was surrounded by lamellar bone. These findings show that, whereas unloaded jaws resembled the normal osteoporotic microarchitecture after one year without loading, the BCP assisted in preserving a proper microarchitecture after seven years. Hence, the authors concluded that BCP 3D-printed scaffolds are an appropriate alternative for bone regeneration: they may lead to more straightforward and less time-consuming surgery, as well as bone preservation [245].

Considering admitted clinical trials, there are valid reports on utilizing some porous ceramic bone scaffolds used to restitute the bone tissue [191,246] (Fig. 10a-d). Studies in the clinical use of BCP scaffolds in bone substitutes are going on [247,248]. Also, the use of commercial BCP-based bone grafts (Fig. 10e-g) is increasing. Uzeda *et al.* [192] studied the effect of various composition ratios of HA: β-TCP in the BCP scaffolds on the clinical responses of BCP in fresh dental sockets after three and six months in a randomized clinical trial. They evaluated histological and histomorphometric responses, focusing on fibrous connective tissue and newly formed bone around the regenerated area. The newly formed bone in the alveolar defect area filled with HA: β-TCP scaffolds with the composition of 60.28: 39.72 and 78.21: 21.79 was reported to be 69.3% ± 6.03% and 46.6% ± 7.66%, respectively [192]. They concluded that scaffolds with the HA: β-TCP composition ratio of 60.28: 39.72 showed a more considerable amount of newly formed bone after six months.

Overall, BCPs are now widely recommended for bone tissue substitutes in bone reconstructive surgery. Among the various clinical studies in the literature proving the efficacy of BCPs [74,249-252], Passuti *et al.* [253] and Randsford *et al.* [78] investigations played a crucial role in the development and approval of BCPs. Considering clinical trial studies, BCP's dramatic role in bone regeneration was confirmed [254-256]. From where we are standing, using AM techniques to fabricate BCP bone scaffolds would be hanging on until clinics are equipped with a printer and related instruments [257]. The bench to the bedside procedure in this area would be promoted by more commercialization of BCP constructs soon.

Conclusions

The present paper reviewed the potentials, applications, evaluations, and challenges of Biphasic Calcium Phosphate bone scaffolds fabricated by the robocasting technique. Considering the advantages and disadvantages, it could be concluded that robocasting is a suitable technique to produce porous scaffolds supporting cell viability, proliferation, and differentiation. Observations in the experiments show a decrease in the compressive strength of robocasted scaffolds by increasing the porosity volume. As pore size and porosities in the scaffolds should be similar to the ingrowing trabecular bone, choosing the proper porosity rate is essential. Although playing a vital role in bone tissue growth and some metabolic activities, such as vascularization, Oxygen delivery, growth factors, and cell nutrition, porosities would negatively affect strength.

HA and especially BCP scaffolds possess significantly higher cell growth and proliferation rate based on ALP activity and collagen I content than β-TCP scaffolds. Extruded scaffolds have a precise, controlled internal architecture with programable interconnectivity, controllable porosity, and various structure, loading a variety of drugs and growth factors are possible. Since mentioned advantages could accelerate delivering the drug, growth factor, and nutrients to the cells, the robocasted scaffolds could improve the tissue growth and formation. The optimum composition ratio of 60 HA/40 β-TCP has an elevated effect on bone fracture regeneration capability with appropriate mechanical performance, while greater bone induction and biological properties require a higher amount of β-TCP. Considering its challenges and struggles, BCP could be appropriately used as a bone substituting material as a corollary. It seems that utilizing AM techniques to fabricate BCP bone scaffolds would be hanging on until clinics are equipped with a printer and related instruments in the near future. The bench to the bedside procedure in this area would be promoted by more commercialization of BCP constructs soon.

Funding

This study was not funded by any institute.

Declaration of Competing Interest

The authors declare that they have no known competing financial interests or personal relationships that could have appeared to influence the work reported in this paper.

References

[1] Roco MC, Bainbridge WS. Converging technologies for improving human performance: integrating from the nanoscale. J Nanoparticle Res 2002;4(4):281–95.
[2] Buikema JW, Van Der Meer P, Sluijter JPG, Domian IJ. Concise review: engineering myocardial tissue: the convergence of stem cells biology and tissue engineering technology. Stem Cells 2013;31(12):2587–98.
[3] Amini AR, Laurencin CT, Nukavarapu SP. Bone tissue engineering: recent advances and challenges. Crit Rev Biomed Eng 2012;40(5):363–408.
[4] Costantini S, Conte C. Bone health in diabetes and prediabetes. World J Diabetes 2019;10(8):421–45.
[5] Hench LL, Polak JM. Third-generation biomedical materials. Science (New York, NY) 2002;295(5557):1014–7.
[6] Wei F-C, Seah C-S, Tsai Y-C, Liu S-J, Tsai M-S. Fibula osteoseptocutaneous flap for reconstruction of composite mandibular defects. Plast Reconstr Surg 1994;93(2).
[7] Vidal L, Kampleitner C, Brennan MÁ, Hoornaert A, Layrolle P. Reconstruction of large skeletal defects: current clinical therapeutic strategies and future directions using 3D printing. Front Bioeng Biotechnol 2020;8. 61-61.
[8] Fernandez de Grado G, Keller L, Idoux-Gillet Y, Wagner Q, Musset A-M, Benkirane-Jessel N, et al. Bone substitutes: a review of their characteristics, clinical use, and perspectives for large bone defects management 2041731418776819. J Tissue Eng 2018;9.
[9] Farzin A, Fathi M, Emadi R. Multifunctional magnetic nanostructured hardystonite scaffold for hyperthermia, drug delivery and tissue engineering applications. Mater Sci Eng, C 2017;70:21–31.
[10] Navarro M, Michiardi A, Castaño O, Planell JA. Biomaterials in orthopaedics. J R Soc Interface 2008;5(27):1137–58.
[11] Sun W, Lal P. Recent development on computer aided tissue engineering–a review. Comput Methods Programs Biomed 2002;67(2):85–103.
[12] Ewais AMMAaEMM. Bioceramic Scaffolds, in Scaffolds in Tissue Engineering - Materials, Technologies and Clinical Applications, Francesco Baino, Editor. 2017, IntechOpen.
[13] Liu X, Ma PX. Polymeric scaffolds for bone tissue engineering. Ann Biomed Eng 2004;32(3):477–86.
[14] Duan B, Wang M. Customized Ca-P/PHBV nanocomposite scaffolds for bone tissue engineering: design, fabrication, surface modification and sustained release of growth factor. J R Soc Interface 2010;7 Suppl 5(Suppl 5):S615–29.
[15] O'Brien FJ. Biomaterials & scaffolds for tissue engineering. Mater Today 2011;14(3):88–95.
[16] Williams JM, Adewunmi A, Schek RM, Flanagan CL, Krebsbach PH, Feinberg SE, et al. Bone tissue engineering using polycaprolactone scaffolds fabricated via selective laser sintering. Biomaterials 2005;26(23):4817–27.
[17] Johari B, Ahmadzadehzarajabad M, Azami M, Kazemi M, Soleimani M, Kargozar S, et al. Repair of rat critical size calvarial defect using osteoblast-like and umbilical vein endothelial cells seeded in gelatin/hydroxyapatite scaffolds. J Biomed Mater Res Part A 2016;104(7):1770–8.
[18] Bose S, Vahabzadeh S, Bandyopadhyay A. Bone tissue engineering using 3D printing. Mater Today 2013;16(12):496–504.
[19] Chen F-M, Liu X. Advancing biomaterials of human origin for tissue engineering. Prog Polym Sci 2016;53:86–168.
[20] Pina S, Ribeiro VP, Marques CF, Maia FR, Silva TH, Reis RL, et al. Scaffolding strategies for tissue engineering and regenerative medicine applications. Materials (Basel) 2019;12(11):1824.
[21] Beheshtizadeh N, Lotfibakhshaiesh N, Pazhouhnia Z, Hoseinpour M, Nafari M. A review of 3D bio-printing for bone and skin tissue engineering: a commercial approach. J Mater Sci 2020;55(9):3729–49.
[22] Böhm AM, Dirckx N, Maes C. Rekrutierung osteogener Zellen an den Ort der Knochenbildung während Entwicklung und Frakturheilung. Z Rheumatol 2016;75(3):316–21.
[23] Zubeldia-Brenner L, Roselli CE, Recabarren SE, Gonzalez Deniselle MC, Lara HE. Developmental and functional effects of steroid hormones on the neuroendocrine axis and spinal cord. J Neuroendocrinol 2016;28(7).
[24] Katagiri T, Tsukamoto S, Kuratani M. Heterotopic bone induction via BMP signaling: Potential therapeutic targets for fibrodysplasia ossificans progressiva. Bone 2018;109:241–50.
[25] Kashte S, Jaiswal AK, Kadam S. Artificial bone via bone tissue engineering: current scenario and challenges. Tissue Eng Regen Med 2017;14(1):1–14.
[26] Feng X. Chemical and biochemical basis of cell-bone matrix interaction in health and disease. Curr Chem Biol 2009;3(2):189–96.
[27] Filippi M, Born G, Chaaban M, Scherberich A. Natural polymeric scaffolds in bone regeneration. Front Bioeng Biotechnol 2020;8:474.
[28] Koons GL, Diba M, Mikos AG. Materials design for bone-tissue engineering. Nat Rev Mater 2020;5(8):584–603.
[29] Probst FA, Fliefel R, Burian E, Probst M, Eddicks M, Cornelsen M, et al. Bone regeneration of minipig mandibular defect by adipose derived mesenchymal stem cells seeded tri-calcium phosphate- poly(D, L-lactide-co-glycolide) scaffolds. Sci Rep 2020;10(1):2062.
[30] Jahan K, Manickam G, Tabrizian M, Murshed M. In vitro and in vivo investigation of osteogenic properties of self-contained phosphate-releasing injectable purine-crosslinked chitosan-hydroxyapatite constructs. Sci Rep 2020;10(1):11603.
[31] D. Iannazzo, A. Pistone, M. Salamò, S. Galvagno, 6 - Hybrid ceramic/polymer composites for bone tissue regeneration, in: V.K. Thakur, M.K. Thakur, R.K.

Gupta (Eds.), Hybrid Polymer Composite Materials, Woodhead Publishing, 2017, pp. 125-155
[32] Grémare A, Guduric V, Bareille R, Heroguez V, Latour S, L'Heureux N, et al. Characterization of printed PLA scaffolds for bone tissue engineering. J Biomed Mater Res A 2018;106(4):887–94.
[33] Rodrigues N, Benning M, Ferreira AM, Dixon L, Dalgarno K. Manufacture and characterisation of porous PLA scaffolds. Procedia CIRP 2016;49:33–8.
[34] Gentile P, Chiono V, Carmagnola I, Hatton PV. An overview of poly(lactic-co-glycolic) Acid (PLGA)-based biomaterials for bone tissue engineering. Int J Mol Sci 2014;15(3):3640–59.
[35] Wu Y-C, Shaw S-Y, Lin H-R, Lee T-M, Yang C-Y. Bone tissue engineering evaluation based on rat calvaria stromal cells cultured on modified PLGA scaffolds. Biomaterials 2006;27(6):896–904.
[36] Nitya G, Nair GT, Mony U, Chennazhi KP, Nair SV. In vitro evaluation of electrospun PCL/nanoclay composite scaffold for bone tissue engineering. J Mater Sci: Mater Med 2012;23(7):1749–61.
[37] Park SA, Lee SH, Kim WD. Fabrication of porous polycaprolactone/hydroxyapatite (PCL/HA) blend scaffolds using a 3D plotting system for bone tissue engineering. Bioprocess Biosyst Eng 2011;34(4):505–13.
[38] Shor L, Güçeri S, Chang R, Gordon J, Kang Q, Hartsock L, et al. Precision extruding deposition (PED) fabrication of polycaprolactone (PCL) scaffolds for bone tissue engineering. Biofabrication 2009;1(1):015003.
[39] Yoshikawa H, Myoui A. Bone tissue engineering with porous hydroxyapatite ceramics. J Artif Organs 2005;8(3):131–6.
[40] Zhou H, Lee J. Nanoscale hydroxyapatite particles for bone tissue engineering. Acta Biomater 2011;7(7):2769–81.
[41] Farzin A, Ahmadian M, Fathi MH. Comparative evaluation of biocompatibility of dense nanostructured and microstructured Hydroxyapatite/Titania composites. Mater Sci Eng, C 2013;33(4):2251–7.
[42] Fang Geng LT, Bingchun Zhang, Chunfu Wu, Yonglian He, Jingyu Yang, Ke Yang. Study on b-TCP coated porous mg as a bone tissue engineering scaffold material. J Mater Sci Technol, 2009. 25(01): p. 123-129
[43] Gao P, Zhang H, Liu Y, Fan B, Li X, Xiao X, et al. Beta-tricalcium phosphate granules improve osteogenesis in vitro and establish innovative osteo-regenerators for bone tissue engineering in vivo. Sci Rep 2016;6:23367.
[44] Kazemi M, Dehghan MM, Azami M. Biological evaluation of porous nanocomposite scaffolds based on strontium substituted β-TCP and bioactive glass: An in vitro and in vivo study. Mater Sci Eng C Mater Biol Appl 2019;105:110071.
[45] Celikkin N, Mastrogiacomo S, Jaroszewicz J, Walboomers XF, Swieszkowski W. Gelatin methacrylate scaffold for bone tissue engineering: The influence of polymer concentration. J Biomed Mater Res A 2018;106(1):201–9.
[46] Sun M, Sun X, Wang Z, Guo S, Yu G, Yang H. Synthesis and properties of gelatin methacryloyl (GelMA) hydrogels and their recent applications in load-bearing tissue. Polymers 2018;10(11):1290.
[47] Bakhtiari L, Rezaie HR, Hosseinalipour SM, Shokrgozar MA. Investigation of biphasic calcium phosphate/gelatin nanocomposite scaffolds as a bone tissue engineering. Ceram Int 2010;36(8):2421–6.
[48] Nery EB, LeGeros RZ, Lynch KL, Lee K. Tissue response to biphasic calcium phosphate ceramic with different ratios of HA/βTCP in periodontal osseous defects. J Periodontol 1992;63(9):729–35.
[49] Ramay HRR, Zhang M. Biphasic calcium phosphate nanocomposite porous scaffolds for load-bearing bone tissue engineering. Biomaterials 2004;25(21):5171–80.
[50] Baheiraei N, Nourani MR, Mortazavi SMJ, Movahedin M, Eyni H, Bagheri F, et al. Development of a bioactive porous collagen/β-tricalcium phosphate bone graft assisting rapid vascularization for bone tissue engineering applications. J Biomed Mater Res A 2018;106(1):73–85.
[51] Bhaskar B, Owen R, Bahmaee H, Wally Z, Sreenivasa Rao P, Reilly GC. Composite porous scaffold of PEG/PLA support improved bone matrix deposition in vitro compared to PLA-only scaffolds. J Biomed Mater Res A 2018;106(5):1334–40.
[52] Turnbull G, Clarke J, Picard F, Riches P, Jia L, Han F, et al. 3D bioactive composite scaffolds for bone tissue engineering. Bioact Mater 2018;3(3):278–314.
[53] Zhang H, Mao X, Du Z, Jiang W, Han X, Zhao D, et al. Three dimensional printed macroporous polylactic acid/hydroxyapatite composite scaffolds for promoting bone formation in a critical-size rat calvarial defect model. Sci Technol Adv Mater 2016;17(1):136–48.
[54] Tavakol S, Azami M, Khoshzaban A, Ragerdi Kashani I, Tavakol B, Hoveizi E, et al. Effect of laminated hydroxyapatite/gelatin nanocomposite scaffold structure on osteogenesis using unrestricted somatic stem cells in rat. Cell Biol Int 2013;37(11):1181–9.
[55] Wang P, Zhao L, Liu J, Weir MD, Zhou X, Xu HHK. Bone tissue engineering via nanostructured calcium phosphate biomaterials and stem cells. Bone Res 2014;2(1):14017.
[56] Eliaz N, Metoki N. Calcium phosphate bioceramics: a review of their history, structure, properties, coating technologies and biomedical applications. Materials (Basel) 2017;10(4):334.
[57] Hao Z, Janak Lal P, Yusheng S, Jiabing R, Liang L, Qi Y, et al. Indirect selective laser sintering printed microporous biphasic calcium phosphate scaffold promotes endogenous bone regeneration via activation of ERK1/2 signaling. Biofabrication 2020.
[58] Zhang C, Yang F, Xiao D, Zhao Q, Chen S, Liu K, et al. Repair of segmental rabbit radial defects with Cu/Zn co-doped calcium phosphate scaffolds incorporating GDF-5 carrier. RSC Adv 2020;10(4):1901–9.
[59] Baheiraei N, Azami M, Hosseinkhani H. Investigation of magnesium incorporation within gelatin/calcium phosphate nanocomposite scaffold for bone tissue engineering. Int J Appl Ceram Technol 2015;12(2):245–53.
[60] Tabatabaee S, Najafi-Ashtiani M, Mousavi A, Baheiraei N. Chapter 2 - Nanobiomaterials in musculoskeletal regeneration. In: Razavi M, editor, Nanoengineering in Musculoskeletal Regeneration. Academic Press; 2020. p. 43-76.
[61] Khoshniat S, Bourgine A, Julien M, Weiss P, Guicheux J, Beck L. The emergence of phosphate as a specific signaling molecule in bone and other cell types in mammals. Cell Mol Life Sci 2011;68(2):205–18.
[62] Nguyen TBL, Lee B-T. A combination of biphasic calcium phosphate scaffold with hyaluronic acid-gelatin hydrogel as a new tool for bone regeneration. Tissue Eng Part A 2014;20(13–14):1993–2004.
[63] Castilho M, Moseke C, Ewald A, Gbureck U, Groll J, Pires I, et al. Direct 3D powder printing of biphasic calcium phosphate scaffolds for substitution of complex bone defects. Biofabrication 2014;6(1):015006.
[64] Jiménez M, Romero L, Domínguez IA, Espinosa MdM, Domínguez M. Additive manufacturing technologies: an overview about 3D printing methods and future prospects. Complexity, 2019; 2019: p. 9656938.
[65] Sa MW, Nguyen BNB, Moriarty RA, Kamalitdinov T, Fisher JP, Kim JY. Fabrication and evaluation of 3D printed BCP scaffolds reinforced with ZrO2 for bone tissue applications. Biotechnol Bioeng 2018;115(4):989–99.
[66] Kasch S, Dowling M. Commercialization strategies of young biotechnology firms: An empirical analysis of the U.S. industry. Res Policy 2008;37(10):1765–77.
[67] Ebrahimian-Hosseinabadi M, Ashrafizadeh F, Etemadifar M, Venkatraman SS. Evaluating and modeling the mechanical properties of the prepared PLGA/nano-BCP composite scaffolds for bone tissue engineering. J Mater Sci Technol 2011;27(12):1105–12.
[68] Miramond T, Borget P, Baroth S, Guy D. Comparative critical study of commercial calcium phosphate bone substitutes in terms of physic-chemical properties. Key Eng Mater 2014;587:63–8.
[69] Ku J-K, Hong I, Lee B-K, Yun P-Y, Lee JK. Dental alloplastic bone substitutes currently available in Korea. J Korean Assoc Oral Maxillofac Surg 2019;45(2):51–67.
[70] Baiomy AABA. Effect of Osteon II Collagen with Hyaluronic Acid on Osseointegration of simultaneous placed implant in piezoelectric splitted posterior mandibular alveolar ridge (Clinical and radiographic study). Egyptian Dental J, 2019; 65(Issue 1 - January (Oral Surgery)): p. 103-112.
[71] Miramond T, Corre P, Borget P, Moreau F, Guicheux J, Daculsi G, et al. Osteoinduction of biphasic calcium phosphate scaffolds in a nude mouse model. J Biomater Appl 2014;29(4):595–604.
[72] Piecuch JF. Augmentation of the atrophic edentulous ridge with porous replamineform hydroxyapatite (Interpore-200). Dent Clin North Am 1986;30(2):291–305.
[73] White E, Shors EC. Biomaterial aspects of Interpore-200 porous hydroxyapatite. Dent Clin North Am 1986;30(1):49–67.
[74] Cho D-Y, Lee W-Y, Sheu P-C, Chen C-C. Cage containing a biphasic calcium phosphate ceramic (Triosite) for the treatment of cervical spondylosis. Surg Neurol 2005;63(6):497–503.
[75] Yang DH, Park HN, Bae MS, Lee JB, Heo DN, Lee WJ, et al. Evaluation of GENESIS-BCP™ scaffold composed of hydroxyapatite and β-tricalcium phosphate on bone formation. Macromol Res 2012;20(6):627–33.
[76] Guy D, E.S., Verner C, Kimakhe S. Clinical performance of moldable bioceramics and resorbable membrane for bone and mucosa regeneration in maxillofacial surgery. Biomater Med Appl, 2017. 1(2).
[77] Dupraz A, Nguyen TP, Richard M, Daculsi G, Passuti N. Influence of a cellulosic ether carrier on the structure of biphasic calcium phosphate ceramic particles in an injectable composite material. Biomaterials 1999;20(7):663–73.
[78] Ransford AO, Morley T, Edgar MA, Webb P, Passuti N, Chopin D, et al. Synthetic porous ceramic compared with autograft in scoliosis surgery. A prospective, randomized study of 341 patients. J Bone Joint Surg Br 1998;80(1):13–8.
[79] Henkel J, Hutmacher DW. Design and fabrication of scaffold-based tissue engineering. BioNanoMaterials 2013;14(3–4):171–93.
[80] Prasad A, Sankar MR, Katiyar V. State of art on solvent casting particulate leaching method for orthopedic scaffoldsfabrication. Mater Today Procc, 2017. 4(2, Part A): p. 898-907.
[81] Chen W, Zhou H, Tang M, Weir MD, Bao C, Xu HHK. Gas-foaming calcium phosphate cement scaffold encapsulating human umbilical cord stem cells. Tissue Eng Part A 2012;18(7–8):816–27.
[82] Sultana N, Wang M. Fabrication of HA/PHBV composite scaffolds through the emulsion freezing/freeze-drying process and characterisation of the scaffolds. J Mater Sci - Mater Med 2007;19(7):2555.
[83] Bochicchio B, Barbaro K, De Bonis A, Rau JV, Pepe A. Electrospun poly(d, l-lactide)/gelatin/glass-ceramics tricomponent nanofibrous scaffold for bone tissue engineering. J Biomed Mater Res A 2020;n/a(n/a).
[84] Sedghi R, Shaabani A, Sayyari N. Electrospun triazole-based chitosan nanofibers as a novel scaffolds for bone tissue repair and regeneration. Carbohydr Polym 2020;230:115707.
[85] Akbarzadeh R, Yousefi AM. Effects of processing parameters in thermally induced phase separation technique on porous architecture of scaffolds for bone tissue engineering. J Biomed Mater Res B Appl Biomater 2014;102(6):1304–15.
[86] Piaia L, Salmoria GV, Hotza D. Chapter 10 - Additive manufacturing of nanostructured bone scaffolds. In: Souza JCM, Hotza D, Henriques B, et al.,

Editors. Nanostructured Biomaterials for Cranio-Maxillofacial and Oral Applications. Elsevier; 2018. p. 181-210.
[87] Gorth D, Webster J. T., 10 - Matrices for tissue engineering and regenerative medicine. In: Lysaght M, Webster TJ, Editors. Biomaterials for artificial organs. Woodhead Publishing; 2011. p. 270-286.
[88] Carter P, Bhattarai N. Chapter 7 - bioscaffolds: fabrication and performance. In: Lakhtakia A, Martín-Palma RJ, editors. Engineered biomimicry. Boston: Elsevier; 2013. p. 161–88.
[89] Jose Varghese R, Sakho EhM, Parani S, Thomas S, Oluwafemi OS, Wu J. Chapter 3 - Introduction to nanomaterials: synthesis and applications. In: Thomas S, Sakho EHM, Kalarikkal N, et al., Editors. Nanomaterials for solar cell applications. Elsevier; 2019. p. 75-95.
[90] Huang Z-M, Zhang YZ, Kotaki M, Ramakrishna S. A review on polymer nanofibers by electrospinning and their applications in nanocomposites. Compos Sci Technol 2003;63(15):2223–53.
[91] Wu H, Hu L, Rowell MW, Kong D, Cha JJ, McDonough JR, et al. Electrospun metal nanofiber webs as high-performance transparent electrode. Nano Lett 2010;10(10):4242–8.
[92] Wu H, Pan W, Lin D, Li H. Electrospinning of ceramic nanofibers: Fabrication, assembly and applications. J Adv Ceram 2012;1(1):2–23.
[93] Ji H, Zhao R, Zhang N, Jin C, Lu X, Wang C. Lightweight and flexible electrospun polymer nanofiber/metal nanoparticle hybrid membrane for high-performance electromagnetic interference shielding. NPG Asia Mater 2018;10(8):749–60.
[94] Hekmati AH, Rashidi A, Ghazisaeidi R, Drean J-Y. Effect of needle length, electrospinning distance, and solution concentration on morphological properties of polyamide-6 electrospun nanowebs. Text Res J 2013;83(14):1452–66.
[95] de Castro MDL, García JLL. Chapter 2 - Analytical freeze-drying. In: de Castro MDL, García JLL, Editors. Techniques and instrumentation in analytical chemistry. Elsevier; 2002. p. 11-41.
[96] Robards K, Haddad PR, Jackson PE. 8 - Sample handling in chromatography. In: Robards K, Haddad PR, Jackson PE, editors. Principles and practice of modern chromatographic methods. Boston: Academic Press; 2004. p. 407–55.
[97] Durance T, Yaghmaee P. 4.51 - Microwave dehydration of food and food ingredients, in comprehensive biotechnology (second edition), M. Moo-Young, Editor. 2011, Academic Press: Burlington. p. 617-628.
[98] Ventura RD, Padalhin AR, Kim B, Park M, Lee BT. Evaluation of bone regeneration potential of injectable extracellular matrix (ECM) from porcine dermis loaded with biphasic calcium phosphate (BCP) powder. Mater Sci Eng C 2020;110:110663.
[99] Yuan B, Zhou S-Y, Chen X-S. Rapid prototyping technology and its application in bone tissue engineering. J Zhejiang Univ Sci B 2017;18(4):303–15.
[100] Thavornyutikarn B, Chantarapanich N, Sitthiseripratip K, Thouas GA, Chen Q. Bone tissue engineering scaffolding: computer-aided scaffolding techniques. Prog Biomater 2014;3(2):61–102.
[101] Hammel EC, Ighodaro OLR, Okoli OI. Processing and properties of advanced porous ceramics: An application based review. Ceram Int, 2014. 40(10, Part A): p. 15351-15370.
[102] Studart AR, Gonzenbach UT, Tervoort E, Gauckler LJ. Processing routes to macroporous ceramics: a review. J Am Ceram Soc 2006;89(6):1771–89.
[103] Nam YS, Yoon JJ, Park TG. A novel fabrication method of macroporous biodegradable polymer scaffolds using gas foaming salt as a porogen additive. J Biomed Mater Res 2000;53(1):1–7.
[104] Deville S, Saiz E, Tomsia AP. Freeze casting of hydroxyapatite scaffolds for bone tissue engineering. Biomaterials 2006;27(32):5480–9.
[105] Manam NS, Harun WSW, Shri DNA, Ghani SAC, Kurniawan T, Ismail MH, et al. Study of corrosion in biocompatible metals for implants: A review. J Alloy Compd 2017;701:698–715.
[106] Li Y, Yang C, Zhao H, Qu S, Li X, Li Y. New developments of Ti-based alloys for biomedical applications. Materials (Basel) 2014;7(3):1709–800.
[107] Kaur M, Singh K. Review on titanium and titanium based alloys as biomaterials for orthopaedic applications. Mater Sci Eng C 2019;102:844–62.
[108] Wauthle R, Ahmadi SM, Amin Yavari S, Mulier M, Zadpoor AA, Weinans H, et al. Revival of pure titanium for dynamically loaded porous implants using additive manufacturing. Mater Sci Eng C 2015;54:94–100.
[109] Webster TJ, Ejiofor JU. Increased osteoblast adhesion on nanophase metals: Ti, Ti6Al4V, and CoCrMo. Biomaterials 2004;25(19):4731–9.
[110] Lohmann CH, Schwartz Z, Köster G, Jahn U, Buchhorn GH, MacDougall MJ, et al. Phagocytosis of wear debris by osteoblasts affects differentiation and local factor production in a manner dependent on particle composition. Biomaterials 2000;21(6):551–61.
[111] Yao H, Li J, Li N, Wang K, Li X, Wang J. Surface modification of cardiovascular stent material 316L SS with estradiol-loaded poly (trimethylene carbonate) film for better biocompatibility. Polymers 2017;9(11).
[112] González MB, Saidman SB. Electrodeposition of polypyrrole on 316L stainless steel for corrosion prevention. Corros Sci 2011;53(1):276–82.
[113] Vandenbroucke B, Kruth JP. Selective laser melting of biocompatible metals for rapid manufacturing of medical parts. Rapid Prototyping J 2007;13(4):196–203.
[114] Liu F-H, Lee R-T, Lin W-H, Liao Y-S. Selective laser sintering of bio-metal scaffold. Procedia CIRP 2013;5:83–7.
[115] Viceconti M, Muccini R, Bernakiewicz M, Baleani M, Cristofolini L. Large-sliding contact elements accurately predict levels of bone-implant micromotion relevant to osseointegration. J Biomech 2000;33(12):1611–8.
[116] Wennerberg A. On surface roughness and implant incorporation; 1996.
[117] Isaacson B, Jeyapalina S. Osseointegration: A review of the fundamentals for assuring cementless skeletal fixation. Orthop Res Rev 2014.
[118] Junker R, Dimakis A, Thoneick M, Jansen JA. Effects of implant surface coatings and composition on bone integration: a systematic review. Clin Oral Implants Res 2009;20(Suppl 4):185–206.
[119] Jing W, Zhang M, Jin L, Zhao J, Gao Q, Ren M, et al. Assessment of osteoinduction using a porous hydroxyapatite coating prepared by micro-arc oxidation on a new titanium alloy. International Journal of Surgery 2015;24:51–6.
[120] Drevet R, Fauré J, Sayen S, Marle-Spiess M, El Btaouri H, Benhayoune H. Electrodeposition of biphasic calcium phosphate coatings with improved dissolution properties. Mater Chem Phys 2019;236:121797.
[121] Wang Z, Huang C, Wang J, Zou B. Development of a novel aqueous hydroxyapatite suspension for stereolithography applied to bone tissue engineering. Ceram Int 2019;45(3):3902–9.
[122] Mangano C, Mangano F, Gobbi L, Admakin O, Iketani S, Giuliani A. Comparative study between laser light stereo-lithography 3D-printed and traditionally sintered biphasic calcium phosphate scaffolds by an integrated morphological, morphometric and mechanical analysis. Int J Mol Sci 2019;20(13).
[123] Ramu M, Ananthasubramanian M, Kumaresan T, Gandhinathan R, Jothi S. Optimization of the configuration of porous bone scaffolds made of Polyamide/Hydroxyapatite composites using Selective Laser Sintering for tissue engineering applications. Biomed Mater Eng 2018;29(6):739–55.
[124] Du Y, Liu H, Yang Q, Wang S, Wang J, Ma J, et al. Selective laser sintering scaffold with hierarchical architecture and gradient composition for osteochondral repair in rabbits. Biomaterials 2017;137:37–48.
[125] Jiao Z, Luo B, Xiang S, Ma H, Yu Y, Yang W. 3D printing of HA / PCL composite tissue engineering scaffolds. Adv Ind Eng Polym Res 2019;2(4):196–202.
[126] Korpela J, Kokkari A, Korhonen H, Malin M, Närhi T, Seppälä J. Biodegradable and bioactive porous scaffold structures prepared using fused deposition modeling. J Biomed Mater Res Part B Appl Biomater 2013;101B(4):610–9.
[127] Du W, Ren X, Pei Z, Ma C. Ceramic binder jetting additive manufacturing: a literature review on density. J Manuf Sci Eng 2020;142(4).
[128] Lv X, Ye F, Cheng L, Fan S, Liu Y. Binder jetting of ceramics: Powders, binders, printing parameters, equipment, and post-treatment. Ceram Int 2019;45(10):12609–24.
[129] Selimis A, Farsari M. 3.8 laser-based 3D printing and surface texturing, in comprehensive materials finishing, Hashmi MSJ, Editor. 2017, Elsevier: Oxford. p. 111-136.
[130] Masood SH. 10.04 - Advances in fused deposition modelling. In: Hashmi S, Batalha GF, Van Tyne CJ, et al., editors. Comprehensive materials processing. Elsevier: Oxford; 2014. p. 69-91
[131] Araújo H, Leite M, Ribeiro AR, Deus AM, Reis L, Vaz MF. The effect of geometry on the flexural properties of cellular core structures. P I Mech Eng L-J Mat 2018;233(3):338–47.
[132] Sclater N, Chironis NP. Mechanisms and mechanical devices sourcebook. New York: McGraw-Hill; 2001.
[133] Zhang Y, Jarosinski W, Jung Y-G, Zhang J. 2 - Additive manufacturing processes and equipment. In: Zhang J, Jung Y-G, editors. Additive manufacturing. Butterworth-Heinemann; 2018. p. 39-51
[134] Mostafaei A, Elliott AM, Barnes JE, Li F, Tan W, Cramer CL, et al. Binder jet 3D printing – process parameters, materials, properties, and challenges. Prog Mater Sci 2020:100707.
[135] Gibson I, Rosen D, Stucker B. Binder jetting. In: Gibson I, Rosen D, Stucker B, editors. Additive manufacturing technologies: 3D printing, rapid prototyping, and direct digital manufacturing. Springer New York: New York, NY; 2015. p. 205-218.
[136] Zhang X-F, Huang Y, Gao G, Cui X. Current progress in bioprinting. In: Advances in biomaterials for biomedical applications. Springer; 2017. p. 227–59.
[137] Chan BP, Leong KW. Scaffolding in tissue engineering: general approaches and tissue-specific considerations. Eur Spine J 2008;17 Suppl 4(Suppl 4):467–79.
[138] Deliormanlı AM, Atmaca H. Effect of pore architecture on the mesenchymal stem cell responses to graphene/polycaprolactone scaffolds prepared by solvent casting and robocasting. J Porous Mater 2020;27(1):49–61.
[139] Ben-Arfa BAE, Neto AS, Palamá IE, Miranda Salvado IM, Pullar RC, Ferreira JMF. Robocasting of ceramic glass scaffolds: Sol–gel glass, new horizons. J Eur Ceram Soc 2019;39(4):1625–34.
[140] Daguano JKMB, Santos C, Alves MFRP, Lopes da Silva JV, Souza MT, Fernandes. State of the art in the use of bioceramics to elaborate 3D structures using robocasting. Int J Adv Med Biotech, 2019; 2(1): p. 55-70.
[141] Bibb R. 5 - Physical reproduction – rapid prototyping technologies. In: Bibb R, editor. Medical modelling. Woodhead Publishing; 2006. p. 59-96.
[142] Webster JG. The measurement, instrumentation, and sensors handbook. Boca Raton, Fla.: CRC Press published in cooperation with IEEE Press; 1999.
[143] Zhang L, Yang G, Johnson BN, Jia X. Three-dimensional (3D) printed scaffold and material selection for bone repair. Acta Biomater 2019;84:16–33.
[144] Jakus AE, Taylor SL, Geisendorfer NR, Dunand DC, Shah RN. Metallic architectures from 3D-printed powder-based liquid inks. Adv Funct Mater 2015;25(45):6985–95.
[145] Ligon SC, Liska R, Stampfl J, Gurr M, Mülhaupt R. Polymers for 3D printing and customized additive manufacturing. Chem Rev 2017;117(15):10212–90.

[146] Varghese G, Moral M, Castro-García M, López-López JJ, Marín-Rueda JR, Yagüe-Alcaraz V, et al. Fabrication and characterisation of ceramics via low-cost DLP 3D printing. Bol Soc Esp Ceram 2018;57(1):9–18.
[147] Chen Z, Li Z, Li J, Liu C, Lao C, Fu Y, et al. 3D printing of ceramics: A review. J Eur Ceram Soc 2019;39(4):661–87.
[148] Maeng W-Y, Jeon J-W, Lee J-B, Lee H, Koh Y-H, Kim H-E. Photocurable ceramic/monomer feedstocks containing terpene crystals as sublimable porogen for UV curing-assisted 3D plotting. J Eur Ceram Soc 2020.
[149] Peng E, Zhang D, Ding J. Ceramic robocasting: recent achievements, potential, and future developments. Adv Mater 2018;30(47):1802404.
[150] Wang Y, Wang K, Li X, Wei Q, Chai W, Wang S, et al. 3D fabrication and characterization of phosphoric acid scaffold with a HA/beta-TCP weight ratio of 60:40 for bone tissue engineering applications. PLoS One, 2017;12(4): p. e0174870.
[151] Munaz A, Vadivelu RK, St. John J, Barton M, Kamble H, Nguyen N-T. Three-dimensional printing of biological matters. J Sci-Adv Mater Dev, 2016; 1(1): p. 1-17.
[152] Jariwala SH, Lewis GS, Bushman ZJ, Adair JH, Donahue HJ. 3D printing of personalized artificial bone scaffolds. 3D Print Addit Manuf 2015;2(2):56–64.
[153] Tappa K, Jammalamadaka U. Novel biomaterials used in medical 3D printing techniques. J Funct Biomater 2018;9(1):17.
[154] Seitz H, Deisinger U, Leukers B, Detsch R, Ziegler G. Different calcium phosphate granules for 3-D printing of bone tissue engineering scaffolds. Adv Eng Mater 2009;11(5):B41–6.
[155] Hamidi A, Tadesse Y. 3D printing of very soft elastomer and sacrificial carbohydrate glass/elastomer structures for robotic applications. Mater Des 2020;187:108324.
[156] Yin P, Hu B, Yi L, Xiao C, Cao X, Zhao L, et al. Engineering of removing sacrificial materials in 3D-printed microfluidics. Micromachines (Basel) 2018;9(7):327.
[157] Franco J, Hunger P, Launey ME, Tomsia AP, Saiz E. Direct write assembly of calcium phosphate scaffolds using a water-based hydrogel. Acta Biomater 2010;6(1):218–28.
[158] Zhao Y, Sun K-N, Wang W-L, Wang Y-X, Sun X-L, Liang Y-J, et al. Microstructure and anisotropic mechanical properties of graphene nanoplatelet toughened biphasic calcium phosphate composite. Ceram Int 2013;39(7):7627–34.
[159] Peroglio M, Gremillard L, Gauthier C, Chazeau L, Verrier S, Alini M, et al. Mechanical properties and cytocompatibility of poly(ε-caprolactone)-infiltrated biphasic calcium phosphate scaffolds with bimodal pore distribution. Acta Biomater 2010;6(11):4369–79.
[160] Wang Y, Wang K, Li X, Wei Q, Chai W, Wang S, et al. 3D fabrication and characterization of phosphoric acid scaffold with a HA/β-TCP weight ratio of 60:40 for bone tissue engineering applications. PLoS ONE 2017;12(4). e0174870-e174870.
[161] Basu B. Three dimensional porous scaffolds: mechanical and biocompatibility properties. In: Basu B, editor. Biomaterials for musculoskeletal regeneration: concepts. Singapore: Springer Singapore; 2017. p. 353–84.
[162] Lewis R. Powder Binder Interactions in 3D inkjet printing; 2014.
[163] Egorov A, Fedotov A, Mironov A, Komlev V, Popov V, Zobkov Y. 3D printing of mineral–polymer bone substitutes based on sodium alginate and calcium phosphate. Beilstein J Nanotechnol 2016;7:1794–9.
[164] Ji A, Zhang S, Bhagia S, Yoo CG, Ragauskas AJ. 3D printing of biomass-derived composites: application and characterization approaches. RSC Adv 2020;10(37):21698–723.
[165] Zhou H, Hou S, Zhang M, Chai H, Liu Y, Bhaduri SB, et al. Synthesis of β-TCP and CPP containing biphasic calcium phosphates by a robust technique. Ceram Int 2016;42(9):11032–8.
[166] Ramezani S, Emadi R, Kharaziha M, Tavangarian F. Synthesis, characterization and in vitro behavior of nanostructured diopside/biphasic calcium phosphate scaffolds. Mater Chem Phys 2017;186:415–25.
[167] Dasgupta S, Tarafder S, Bandyopadhyay A, Bose S. Effect of grain size on mechanical, surface and biological properties of microwave sintered hydroxyapatite. Mater Sci Eng C 2013;33(5):2846–54.
[168] Schumacher M, Uhl F, Detsch R, Deisinger U, Ziegler G. Static and dynamic cultivation of bone marrow stromal cells on biphasic calcium phosphate scaffolds derived from an indirect rapid prototyping technique. J Mater Sci Mater Med 2010;21(11):3039–48.
[169] Petit C, Meille S, Maire E, Gremillard L, Adrien J, Lau GY, et al. Fracture behavior of robocast HA/β-TCP scaffolds studied by X-ray tomography and finite element modeling. J Eur Ceram Soc 2017;37(4):1735–45.
[170] Richard RC, Oliveira RN, Soares GDA, Thiré RMSM. Direct-write assembly of 3D scaffolds using colloidal calcium phosphates inks. Materia 2014;19:61–7.
[171] Touri M, Moztarzadeh F, Osman NAA, Dehghan MM, Mozafari M. 3D-printed biphasic calcium phosphate scaffolds coated with an oxygen generating system for enhancing engineered tissue survival. Mater Sci Eng C 2018;84:236–42.
[172] Touri M, Moztarzadeh F, Osman NAA, Dehghan MM, Mozafari M. Breathable tissue engineering scaffolds: An efficient design-optimization by additive manufacturing. Mater Today Procc 2018;5(7, Part 3):15813–20.
[173] Touri M, Moztarzadeh F, Osman NAA, Dehghan MM, Mozafari M. Optimisation and biological activities of bioceramic robocast scaffolds provided with an oxygen-releasing coating for bone tissue engineering applications. Ceram Int 2019;45(1):805–16.
[174] Li X, Yuan Y, Liu L, Leung Y-S, Chen Y, Guo Y, et al. 3D printing of hydroxyapatite/tricalcium phosphate scaffold with hierarchical porous structure for bone regeneration. Bio Design Manuf 2020;3(1):15–29.
[175] Liu F, Liu Y, Li X, Wang X, Li D, Chung S, et al. Osteogenesis of 3D printed macro-pore size biphasic calcium phosphate scaffold in rabbit calvaria. J Biomater Appl 2019;33(9):1168–77.
[176] Marques CF, Olhero SM, Torres PM, Abrantes JC, Fateixa S, Nogueira HI, et al. Novel sintering-free scaffolds obtained by additive manufacturing for concurrent bone regeneration and drug delivery: Proof of concept. Mater Sci Eng C 2019;94:426–36.
[177] Marques CF, Perera FH, Marote A, Ferreira S, Vieira SI, Olhero S, et al. Biphasic calcium phosphate scaffolds fabricated by direct write assembly: Mechanical, anti-microbial and osteoblastic properties. J Eur Ceram Soc 2017;37(1):359–68.
[178] Song Y, Lin K, He S, Wang C, Zhang S, Li D, et al. Nano-biphasic calcium phosphate/polyvinyl alcohol composites with enhanced bioactivity for bone repair via low-temperature three-dimensional printing and loading with platelet-rich fibrin. Int J Nanomed 2018;13:505–23.
[179] Detsch R, Schaefer S, Deisinger U, Ziegler G, Seitz H, Leukers B. In vitro-osteoclastic activity studies on surfaces of 3D printed calcium phosphate scaffolds. J Biomater Appl 2011;26(3):359–80.
[180] Miranda P, Pajares A, Saiz E, Tomsia AP, Guiberteau F. Mechanical properties of calcium phosphate scaffolds fabricated by robocasting. J Biomed Mater Res A 2008;85A(1):218–27.
[181] Buj I, Domínguez-Fernández A, Gómez-Gejo A. Effect of printing parameters on dimensional error and surface roughness obtained in direct ink writing (DIW) processes. Materials 2020;13:2157.
[182] Feilden E, García-Tuñón E, Giuliani F, Saiz E, Vandeperre L. Robocasting of structural ceramic parts with hydrogel inks. J Eur Ceram Soc 2016;36.
[183] Bland E, Dréau D, Burg KJ. Overcoming hypoxia to improve tissue-engineering approaches to regenerative medicine. J Tissue Eng Regen Med 2013;7(7):505–14.
[184] Tandara AA, Mustoe TA. Oxygen in wound healing–more than a nutrient. World J Surg 2004;28(3):294–300.
[185] Schumacher M, Deisinger U, Detsch R, Ziegler G. Indirect rapid prototyping of biphasic calcium phosphate scaffolds as bone substitutes: influence of phase composition, macroporosity and pore geometry on mechanical properties. J Mater Sci Mater Med 2010;21(12):3119–27.
[186] Hwang K-S, Choi J-W, Kim J-H, Chung HY, Jin S, Shim J-H, et al. Comparative efficacies of collagen-based 3D printed PCL/PLGA/β-TCP composite block bone grafts and biphasic calcium phosphate bone substitute for bone regeneration. Materials 2017;10(4):421.
[187] Detsch R, Schaefer S, Deisinger U, Ziegler G, Seitz H, Leukers B. In vitro: osteoclastic activity studies on surfaces of 3D printed calcium phosphate scaffolds. J Biomater Appl 2011;26(3):359–80.
[188] Ebrahimian-Hosseinabadi M, Ashrafizadeh F, Etemadifar M, Venkatraman SS. Preparation and mechanical behavior of PLGA/nano-BCP composite scaffolds during in-vitro degradation for bone tissue engineering. Polym Degrad Stab 2011;96(10):1940–6.
[189] Nie L, Chen D, Suo J, Zou P, Feng S, Yang Q, et al. Physicochemical characterization and biocompatibility in vitro of biphasic calcium phosphate/polyvinyl alcohol scaffolds prepared by freeze-drying method for bone tissue engineering applications. Colloids Surf B Biointerfaces 2012;100:169–76.
[190] Arinzeh TL, Tran T, McAlary J, Daculsi G. A comparative study of biphasic calcium phosphate ceramics for human mesenchymal stem-cell-induced bone formation. Biomaterials 2005;26(17):3631–8.
[191] Mangano C, Perrotti V, Shibli JA, Mangano F, Ricci L, Piattelli A, et al. Maxillary sinus grafting with biphasic calcium phosphate ceramics: clinical and histologic evaluation in man. Int J Oral Maxillofac Implants 2013;28(1):51–6.
[192] Uzeda MJ, de Brito Resende RF, Sartoretto SC, Alves ATNN, Granjeiro JM, Calasans-Maia MD. Randomized clinical trial for the biological evaluation of two nanostructured biphasic calcium phosphate biomaterials as a bone substitute. Clin Implant Dent Relat Res 2017;19(5):802–11.
[193] Zhao YH, Zhang M, Liu NX, Lv X, Zhang J, Chen FM, et al. The combined use of cell sheet fragments of periodontal ligament stem cells and platelet-rich fibrin granules for avulsed tooth reimplantation. Biomaterials 2013;34(22):5506–20.
[194] Bi L, Cheng W, Fan H, Pei G. Reconstruction of goat tibial defects using an injectable tricalcium phosphate/chitosan in combination with autologous platelet-rich plasma. Biomaterials 2010;31(12):3201–11.
[195] Naik B, Karunakar P, Jayadev M, Marshal VR. Role of Platelet rich fibrin in wound healing: A critical review. J Conserv Dent 2013;16(4):284–93.
[196] Dohan Ehrenfest DM, Rasmusson L, Albrektsson T. Classification of platelet concentrates: from pure platelet-rich plasma (P-PRP) to leucocyte- and platelet-rich fibrin (L-PRF). Trends Biotechnol 2009;27(3):158–67.
[197] Wu CL, Lee SS, Tsai CH, Lu KH, Zhao JH, Chang YC. Platelet-rich fibrin increases cell attachment, proliferation and collagen-related protein expression of human osteoblasts. Aust Dent J 2012;57(2):207–12.
[198] Dohan Ehrenfest DM, Bielecki T, Jimbo R, Barbé G, Del Corso M, Inchingolo F, et al. Do the fibrin architecture and leukocyte content influence the growth factor release of platelet concentrates? An evidence-based answer comparing a pure platelet-rich plasma (P-PRP) gel and a leukocyte- and platelet-rich fibrin (L-PRF). Curr Pharm Biotechnol 2012;13(7):1145–52.

[199] Strauss F-J, Nasirzade J, Kargarpoor Z, Stähli A, Gruber R. Effect of platelet-rich fibrin on cell proliferation, migration, differentiation, inflammation, and osteoclastogenesis: a systematic review of in vitro studies. Clin Oral Investig 2020;24(2):569–84.

[200] Wang C, Huang W, Zhou Y, He L, He Z, Chen Z, et al. 3D printing of bone tissue engineering scaffolds. Bioact Mater 2020;5(1):82–91.

[201] Askari M, Afzali Naniz M, Kouhi M, Saberi A, Zolfagharian A, Bodaghi M. Recent progress in extrusion 3D bioprinting of hydrogel biomaterials for tissue regeneration: a comprehensive review with focus on advanced fabrication techniques. Biomater Sci 2021.

[202] Nikolova MP, Chavali MS. Recent advances in biomaterials for 3D scaffolds: A review. Bioact Mater 2019;4:271–92.

[203] Yamada S, Heymann D, Bouler JM, Daculsi G. Osteoclastic resorption of calcium phosphate ceramics with different hydroxyapatite/β-tricalcium phosphate ratios. Biomaterials 1997;18(15):1037–41.

[204] Maeno S, Niki Y, Matsumoto H, Morioka H, Yatabe T, Funayama A, et al. The effect of calcium ion concentration on osteoblast viability, proliferation and differentiation in monolayer and 3D culture. Biomaterials 2005;26(23):4847–55.

[205] Titorencu I, Jinga VV, Constantinescu E, Gafencu AV, Ciohodaru C, Manolescu I, et al. Proliferation, differentiation and characterization of osteoblasts from human BM mesenchymal cells. Cytotherapy 2007;9(7):682–96.

[206] Gerstenfeld LC, Cho TJ, Kon T, Aizawa T, Cruceta J, Graves BD, et al. Impaired intramembranous bone formation during bone repair in the absence of tumor necrosis factor-alpha signaling. Cells Tissues Organs 2001;169(3):285–94.

[207] Lu J, Blary MC, Vavasseur S, Descamps M, Anselme K, Hardouin P. Relationship between bioceramics sintering and micro-particles-induced cellular damages. J Mater Sci - Mater Med 2004;15(4):361–5.

[208] Fellah BH, Delorme B, Sohier J, Magne D, Hardouin P, Layrolle P. Macrophage and osteoblast responses to biphasic calcium phosphate microparticles. J Biomed Mater Res Part A 2010;93(4):1588–95.

[209] Silva SN, Pereira MM, Goes AM, Leite MF. Effect of biphasic calcium phosphate on human macrophage functions in vitro. J Biomed Mater Res Part A 2003;65(4):475–81.

[210] Toquet J, Rohanizadeh R, Guicheux J, Couillaud S, Passuti N, Daculsi G, et al. Osteogenic potential in vitro of human bone marrow cells cultured on macroporous biphasic calcium phosphate ceramic. J Biomed Mater Res 1999;44(1):98–108.

[211] Saldaña L, Sánchez-Salcedo S, Izquierdo-Barba I, Bensiamar F, Munuera L, Vallet-Regí M, et al. Calcium phosphate-based particles influence osteogenic maturation of human mesenchymal stem cells. Acta Biomater 2009;5(4):1294–305.

[212] Cordonnier T, Layrolle P, Gaillard J, Langonné A, Sensebé L, Rosset P, et al. 3D environment on human mesenchymal stem cells differentiation for bone tissue engineering. J Mater Sci - Mater Med 2010;21(3):981–7.

[213] Oropallo W, Piegl LA. Ten challenges in 3D printing. Eng Comput, 2016. 32(1): p. 135-148.

[214] M'Barki A, Bocquet L, Stevenson A. Linking rheology and printability for dense and strong ceramics by direct ink writing. Sci Rep 2017;7(1):6017.

[215] Schuurman W, Levett PA, Pot MW, van Weeren PR, Dhert WJ, Hutmacher DW, et al. Gelatin-methacrylamide hydrogels as potential biomaterials for fabrication of tissue-engineered cartilage constructs. Macromol Biosci 2013;13(5):551–61.

[216] Peak CW, Stein J, Gold KA, Gaharwar AK. Nanoengineered colloidal inks for 3D bioprinting. Langmuir 2018;34(3):917–25.

[217] Geisendorfer NR, Shah RN. Effect of polymer binder on the synthesis and properties of 3D-printable particle-based liquid materials and resulting structures. ACS Omega 2019;4(7):12088–97.

[218] Bakarich SE, Panhuis Mih, Beirne S, Wallace GG, Spinks GM. Extrusion printing of ionic–covalent entanglement hydrogels with high toughness. J Mater Chem B, 2013. 1(38): p. 4939-4946.

[219] Panda B, Unluer C, Tan MJ. Extrusion and rheology characterization of geopolymer nanocomposites used in 3D printing. Compos B Eng 2019;176:107290.

[220] Malda J, Visser J, Melchels FP, Jungst T, Hennink WE, Dhert WJ, et al. 25th anniversary article: Engineering hydrogels for biofabrication. Adv Mater 2013;25(36):5011–28.

[221] Sulaiman SB, Keong TK, Cheng CH, Saim AB, Idrus RBH. Tricalcium phosphate/hydroxyapatite (TCP-HA) bone scaffold as potential candidate for the formation of tissue engineered bone. Indian J Med Res 2013;137(6):1093–101.

[222] Bose S, Roy M, Bandyopadhyay A. Recent advances in bone tissue engineering scaffolds. Trends Biotechnol 2012;30(10):546–54.

[223] Qu H, Fu H, Han Z, Sun Y. Biomaterials for bone tissue engineering scaffolds: a review. RSC Adv 2019;9(45):26252–62.

[224] Prokopiev O, Sevostianov I. Dependence of the mechanical properties of sintered hydroxyapatite on the sintering temperature. Mater Sci Eng A 2006;431(1):218–27.

[225] Chu K-T, Ou S-F, Chen S-Y, Chiou S-Y, Chou H-H, Ou K-L. Research of phase transformation induced biodegradable properties on hydroxyapatite and tricalcium phosphate based bioceramic. Ceram Int 2013;39(2):1455–62.

[226] Putlyaev VI, Safronova TV. Chemical transformations of calcium phosphates during production of ceramic materials on their basis. Inorg Mater 2019;55(13):1328–41.

[227] Dellinger JG, Wojtowicz AM, Jamison RD. Effects of degradation and porosity on the load bearing properties of model hydroxyapatite bone scaffolds. J Biomed Mater Res A 2006;77A(3):563–71.

[228] Yang HY, Yang SF, Chi XP, Evans JRG, Thompson I, Cook RJ, et al. Sintering behaviour of calcium phosphate filaments for use as hard tissue scaffolds. J Eur Ceram Soc 2008;28(1):159–67.

[229] Dellinger JG, Cesarano III J, Jamison RD. Robotic deposition of model hydroxyapatite scaffolds with multiple architectures and multiscale porosity for bone tissue engineering. J Biomed Mater Res A 2007;82A(2):383–94.

[230] Bose S, Dasgupta S, Tarafder S, Bandyopadhyay A. Microwave-processed nanocrystalline hydroxyapatite: Simultaneous enhancement of mechanical and biological properties. Acta Biomater 2010;6(9):3782–90.

[231] Segre N, Ostertag C, Monteiro PJM. Effect of tire rubber particles on crack propagation in cement paste. Mater Res 2006;9:311–20.

[232] Cho D-G, Yang S-K, Yun J-C, Kim H-S, Lee J-S, Lee CS. Effect of sintering profile on densification of nano-sized Ni/Al2O3 composite. Compos B Eng 2013;45(1):159–64.

[233] Kang Y, Scully A, Young DA, Kim S, Tsao H, Sen M, et al. Enhanced mechanical performance and biological evaluation of a PLGA coated β-TCP composite scaffold for load-bearing applications. Eur Polym J 2011;47(8):1569–77.

[234] Nie L, Suo J, Zou P, Feng S. Preparation and properties of biphasic calcium phosphate scaffolds multiply coated with HA/PLLA nanocomposites for bone tissue engineering applications. J Nanomater 2012;2012:213549.

[235] Farzin A, Hassan S, Moreira Teixeira LS, Gurian M, Crispim JF, Manhas V, et al. Self-oxygenation of tissues orchestrates full-thickness vascularization of living implants. Adv Funct Mater 2021;31(42):2100850.

[236] Peroglio M, Gremillard L, Chevalier J, Chazeau L, Gauthier C, Hamaide T. Toughening of bio-ceramics scaffolds by polymer coating. J Eur Ceram Soc 2007;27(7):2679–85.

[237] Mistry AS, Mikos AG. Tissue engineering strategies for bone regeneration. Adv Biochem Eng Biotechnol 2005;94:1–22.

[238] Sadiasa A, Kim MS, Lee BT. Poly(lactide-co-glycolide acid)/biphasic calcium phosphate composite coating on a porous scaffold to deliver simvastatin for bone tissue engineering. J Drug Target 2013;21(8):719–29.

[239] Fu Q, Jia W, Lau GY, Tomsia AP. Strength, toughness, and reliability of a porous glass/biopolymer composite scaffold. J Biomed Mater Res Part B Appl Biomater, 106(3): 2018; 1209-1217.

[240] Nooeaid P, Li W, Roether JA, Mourino V, Goudouri OM, Schubert DW, et al. Development of bioactive glass based scaffolds for controlled antibiotic release in bone tissue engineering via biodegradable polymer layered coating. Biointerphases 2014;9(4):041001.

[241] Kepa K, Coleman R, Grøndahl L. In vitro mineralization of functional polymers. Biosurf Biotribol 2015;1(3):214–27.

[242] Li J, Liao H, Sjöström M. Characterization of calcium phosphates precipitated from simulated body fluid of different buffering capacities. Biomaterials 1997;18(10):743–7.

[243] Pourmollaabbassi B, Karbasi S, Hashemibeni B. Evaluate the growth and adhesion of osteoblast cells on nanocomposite scaffold of hydroxyapatite/titania coated with poly hydroxybutyrate. Adv Biomed Res 2016;5. 156-156.

[244] Hu J, Zhou Y, Huang L, Liu J, Lu H. Effect of nano-hydroxyapatite coating on the osteoinductivity of porous biphasic calcium phosphate ceramics. BMC Musculoskelet Disord 2014;15(1):114.

[245] Mangano C, Giuliani A, De Tullio I, Raspanti M, Piattelli A, Iezzi G. Case report: histological and histomorphometrical results of a 3-D printed biphasic calcium phosphate ceramic 7 years after insertion in a human maxillary alveolar ridge. Front Bioeng Biotechnol 2021;9:232.

[246] Lin K, Sheikh R, Romanazzo S, Roohani I. 3D printing of bioceramic scaffolds-barriers to the clinical translation: from promise to reality, and future perspectives. Materials (Basel) 2019;12(17):2660.

[247] Sun H, Yang H-L. Calcium phosphate scaffolds combined with bone morphogenetic proteins or mesenchymal stem cells in bone tissue engineering. Chin Med J (Engl) 2015;128(8):1121–7.

[248] Wang W, Yeung KWK. Bone grafts and biomaterials substitutes for bone defect repair: A review. Bioact Mater 2017;2(4):224–47.

[249] Cavagna R, Daculsi G, Bouler JM. Macroporous calcium phosphate ceramic: a prospective study of 106 cases in lumbar spinal fusion. J Long Term Eff Med Implants 1999;9(4):403–12.

[250] Nery EB, Lee KK, Czajkowski S, Dooner JJ, Duggan M, Ellinger RF, et al. A veterans administration cooperative study of biphasic calcium phosphate ceramic in periodontal osseous defects. J Periodontol 1990;61(12):737–44.

[251] Lindgren C, Mordenfeld A, Johansson CB, Hallman M. A 3-year clinical follow-up of implants placed in two different biomaterials used for sinus augmentation. Int J Oral & Maxillofacial Implants 2012;27(5):1151–62.

[252] Delécrin J, Takahashi S, Gouin F, Passuti N. A synthetic porous ceramic as a bone graft substitute in the surgical management of scoliosis: a prospective, randomized study. Spine 2000;25(5):563–9.

[253] Passuti N, Daculsi G, Rogez JM, Martin S, Bainvel JV. Macroporous calcium phosphate ceramic performance in human spine fusion. Clin Orthop Relat Res 1989;248:169–76.

[254] Klimecs V, Grishulonoks A, Salma I, Neimane L, Locs J, Saurina E, et al. Bone loss around dental implants 5 years after implantation of biphasic calcium phosphate (HAp/betaTCP) granules. J Healthc Eng 2018;2018:4804902.

[255] Jain D, Mohan R, Singh VD. Comparison of microsurgical and macrosurgical technique using bioactive synthetic bone graft and collagen membrane for an

implant site development: A randomized controlled clinical trial. J Indian Soc Periodontol 2019;23(5):448–60.
[256] Gomez-Barrena E, Rosset P, Gebhard F, Hernigou P, Baldini N, Rouard H, et al. Feasibility and safety of treating non-unions in tibia, femur and humerus with autologous, expanded, bone marrow-derived mesenchymal stromal cells associated with biphasic calcium phosphate biomaterials in a multicentric, non-comparative trial. Biomaterials 2019;196:100–8.
[257] Do A-V, Khorsand B, Geary SM, Salem AK. 3D printing of scaffolds for tissue regeneration applications. Adv Healthcare Mater 2015;4(12):1742–62.
[258] Naveen Kumar M, Rama Raju B, Sreenivasa Rao P. Study on osteoblast like behavior of umbilical cord blood cells on various combinations of PLGA scaffolds prepared by salt fusion. Curr Stem Cell Res Ther 2013;8(3):253–9.
[259] Barbetta A, Rizzitelli G, Bedini R, Pecci R, Dentini M. Porous gelatin hydrogels by gas-in-liquid foam templating. Soft Matter 2010;6(8):1785–92.
[260] Honarpardaz A, Irani S, Pezeshki-Modaress M, Zandi M, Sadeghi A. Enhanced chondrogenic differentiation of bone marrow mesenchymal stem cells on gelatin/glycosaminoglycan electrospun nanofibers with different amount of glycosaminoglycan. J Biomed Mater Res A 2019;107(1):38–48.
[261] Raucci MG, D'Amora U, Ronca A, Demitri C, Ambrosio L. Bioactivation routes of gelatin-based scaffolds to enhance at nanoscale level bone tissue regeneration. Front Bioeng Biotechnol 2019;7(27).
[262] Samadian H, Farzamfar S, Vaez A, Ehterami A, Bit A, Alam M, et al. A tailored polylactic acid/polycaprolactone biodegradable and bioactive 3D porous scaffold containing gelatin nanofibers and Taurine for bone regeneration. Sci Rep 2020;10(1):13366.
[263] Moxon SR, Ferreira MJS, Santos Pd, Popa B, Gloria A, Katsarava R, et al. A preliminary evaluation of the pro-chondrogenic potential of 3D-bioprinted poly(ester urea) scaffolds. Polymers, 2020. 12(7): p. 1478.
[264] Boccardi E, Philippart A, Juhasz-Bortuzzo JA, Novajra G, Vitale-Brovarone C, Boccaccini AR. Characterisation of Bioglass based foams developed via replication of natural marine sponges. Adv Ceram Prog 2015;114(sup1): S56–62.
[265] Pokhrel A, Seo DN, Lee ST, Kim IJ. Processing of porous ceramics by direct foaming: a review. J Korean Ceram Soc 2013;50(2):93.
[266] Chen L, Deng C, Li J, Yao Q, Chang J, Wang L, et al. 3D printing of a lithium-calcium-silicate crystal bioscaffold with dual bioactivities for osteochondral interface reconstruction. Biomaterials 2019;196:138–50.
[267] Dobrzanski L, Dobrzańska-Danikiewicz A, Gaweł T. Computer-aided design and selective laser melting of porous biomimetic materials. Adv Mater Processing Technol 2016;3:1–13.
[268] Dobrzański LA, Dobrzańska-Danikiewicz AD, Gaweł TG, Achtelik-Franczak A. Selective laser sintering and melting of pristine titanium and titanium Ti6Al4V alloy powders and selection of chemical environment for etching of such materials. Arch Metall Mater 2015;Vol. 60, iss. 3A:2040–5.
[269] Neumann R, Neunzehn J, Hinueber C, Flath T, Schulze FP, Wiesmann HP. 3D-printed poly-ε-caprolactone-CaCO3-biocomposite-scaffolds for hard tissue regeneration. Express Polym Lett 2019;13:2–17.
[270] Mythili Prakasam MP. Roxana Piticescu and Alain Largeteau., Fabrication Methodologies of Biomimetic and Bioactive Scaffolds for Tissue Engineering Applications, in Scaffolds in Tissue Engineering - Materials, Technologies and Clinical Applications, F. Baino, Editor. December 13th 2017, IntechOpen.
[271] Lowmunkong R, Sohmura T, Suzuki Y, Matsuya S, Ishikawa K. Fabrication of freeform bone-filling calcium phosphate ceramics by gypsum 3D printing method. J Biomed Mater Res Part B Appl Biomater 2009;90B(2):531–9.

Nima Beheshtizadeh received his MSc. in mechanical manufacturing engineering. Now, he is completing his Ph.D. program in tissue engineering at Tehran University of Medical Sciences (TUMS). He is interested in tissue engineering, biomaterials, additive manufacturing, and systems biology.

Mahmoud Azami is an associate professor at TUMS. He has received his Ph.D. in biomaterials and his work focuses on the design and preparation of scaffolds for tissue regeneration, especially for bone, skin, and nerve repair using 3D printing techniques.

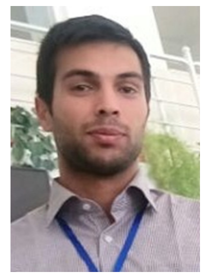

Hossein Abbasi is a university lecturer at Technical and Vocational University in Iran. He received his MSc. in mechanical engineering from University of Tabriz. His research interests are in advanced manufacturing, numerical simulation, and additive manufacturing.

Ali Farzin is an assistant professor at TUMS, Tehran. His scientific activity focuses on the fabrication and characterization of novel bioceramics, multifunctional scaffolds, and oxygen generative biomaterials for cancer therapy, tissue engineering, and drug delivery applications.